Glueball Dark Matter: from Gravitational Waves to Direct Detection

Zhi-Wei Wang 王志伟

Uni. of Electronic Science and Technology of China

May. 7th, 2026

交叉学科理论研究中心、彭桓武高能基础理论研究中心
中国科学技术大学

A Landscape of Phases in QFT (QCD-like Theory) and its Relation to BSM Physics

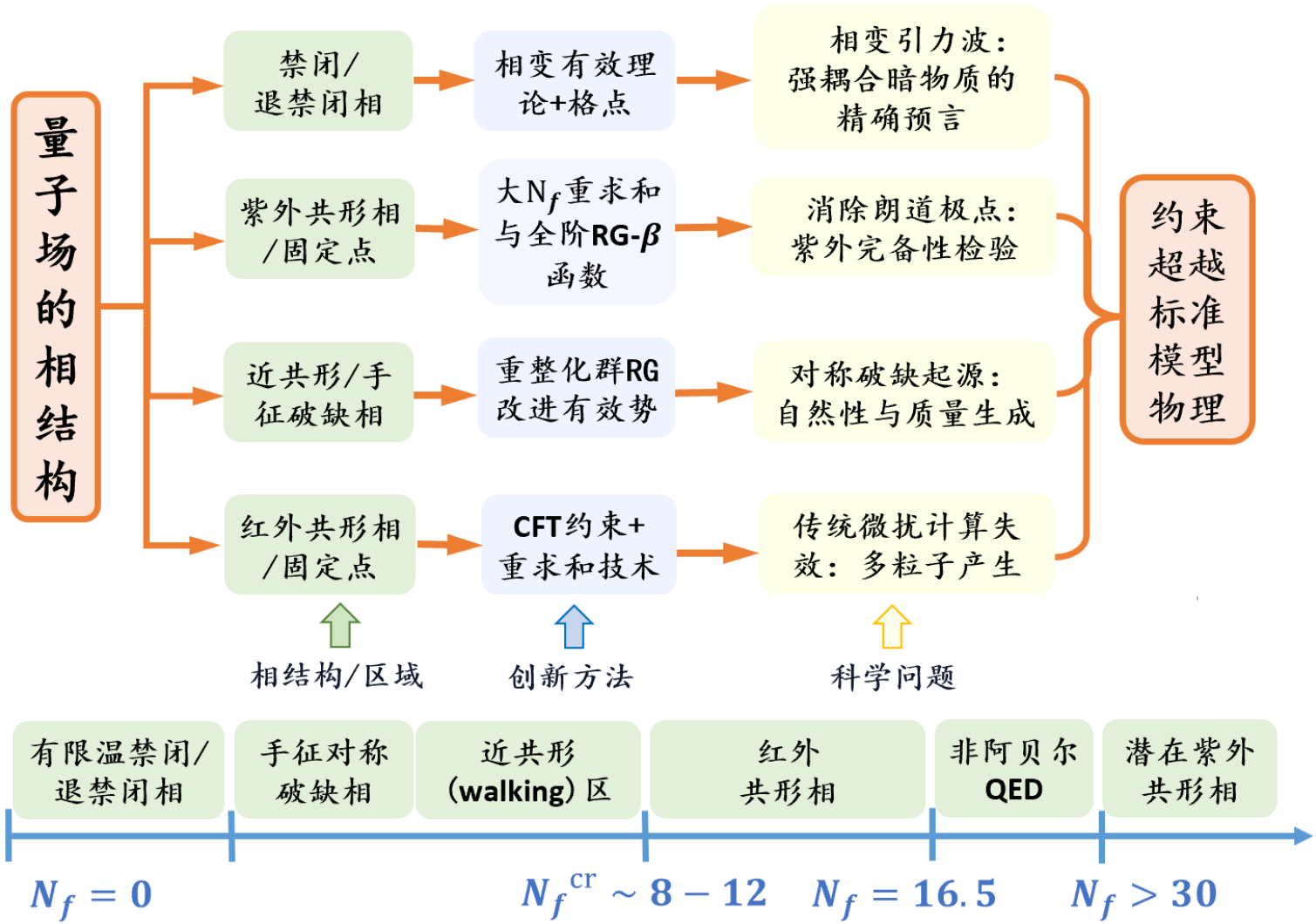

以$SU(N_c)$ $(N_c = 3)$类QCD理论示例，展示随N_f变化的IR/UV行为及固定点结构。

UV Conformal Phase: Asymptotic Safety

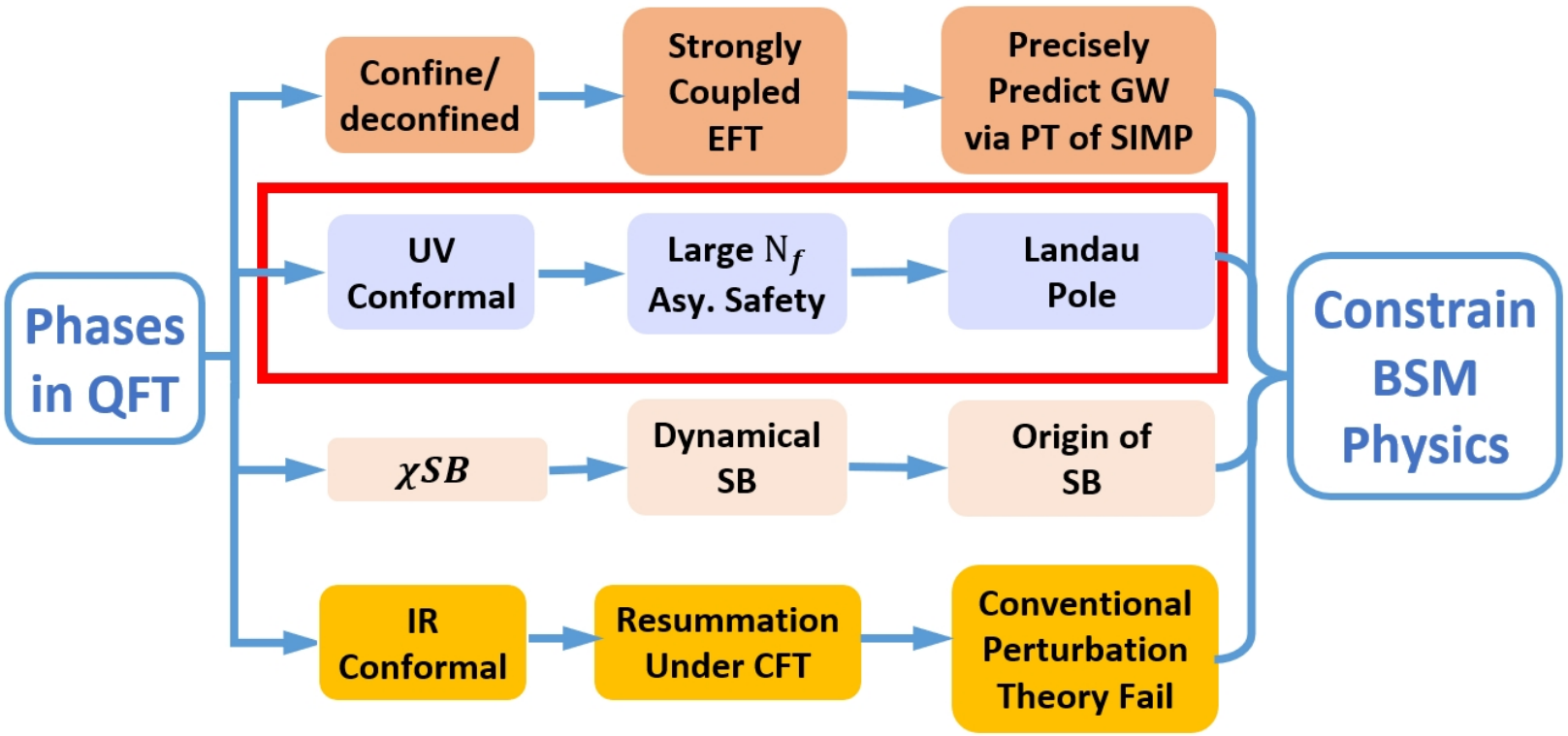

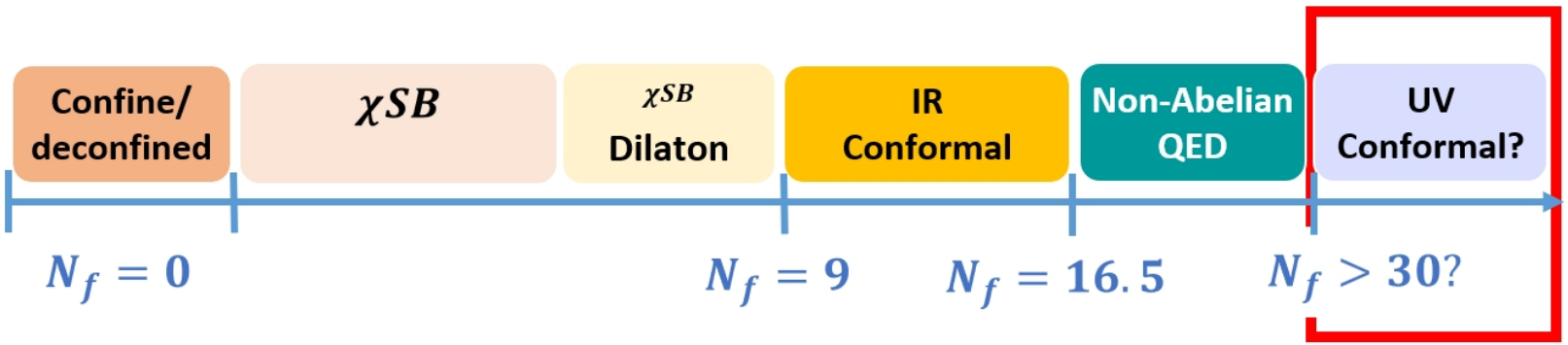

UV phase: Asymptotic Safety

Mann, Meffe, Sannino, Steele, Z-W W and Zhang, Phys. Rev. Lett. 119 (2017) 261802

Antipin, Dondi, Sannino, Thomsen, Z-W W, Phys. Rev. D 98 (2018) 016003

Running, resummation and higher-order structure

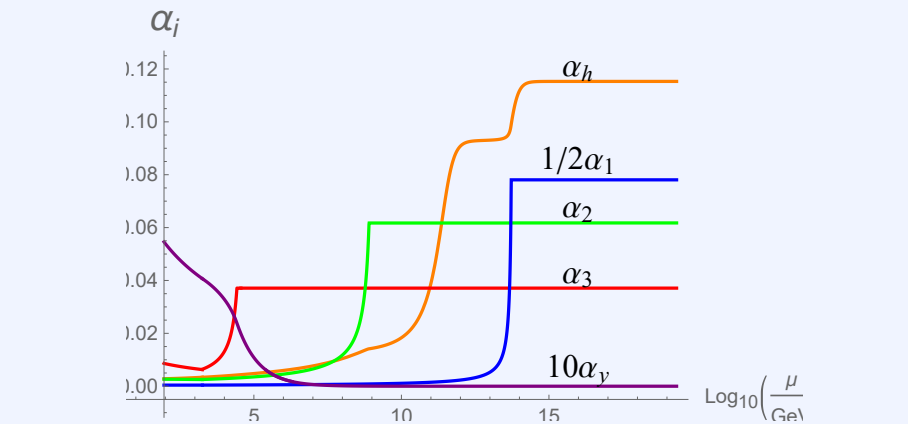

Safe-SM running; resummed $g^2\beta(g^2)$ versus finite-loop truncations; bubble-chain topologies in the large-N_f expansion.

Safe SM and Safe GUTs

- **Safe SM:** vector-like fermions can render $\alpha_{1,2,3}$ and λ_H asymptotically safe; y_t is UV free.
- **Large-N_f RG:** bubble resummation extends to semi-simple gauge groups, Yukawa couplings and scalar quartics.
- **GUT embedding:** Pati-Salam and Trinification embed $U(1)_Y$ into non-Abelian UV-safe dynamics.
- **Predictivity:** UV fixed points act as boundary conditions for Higgs/top matching and BSM model building.

Take-home

Asymptotic safety turns UV completion into predictive IR boundary conditions.

QCD Conformal Window

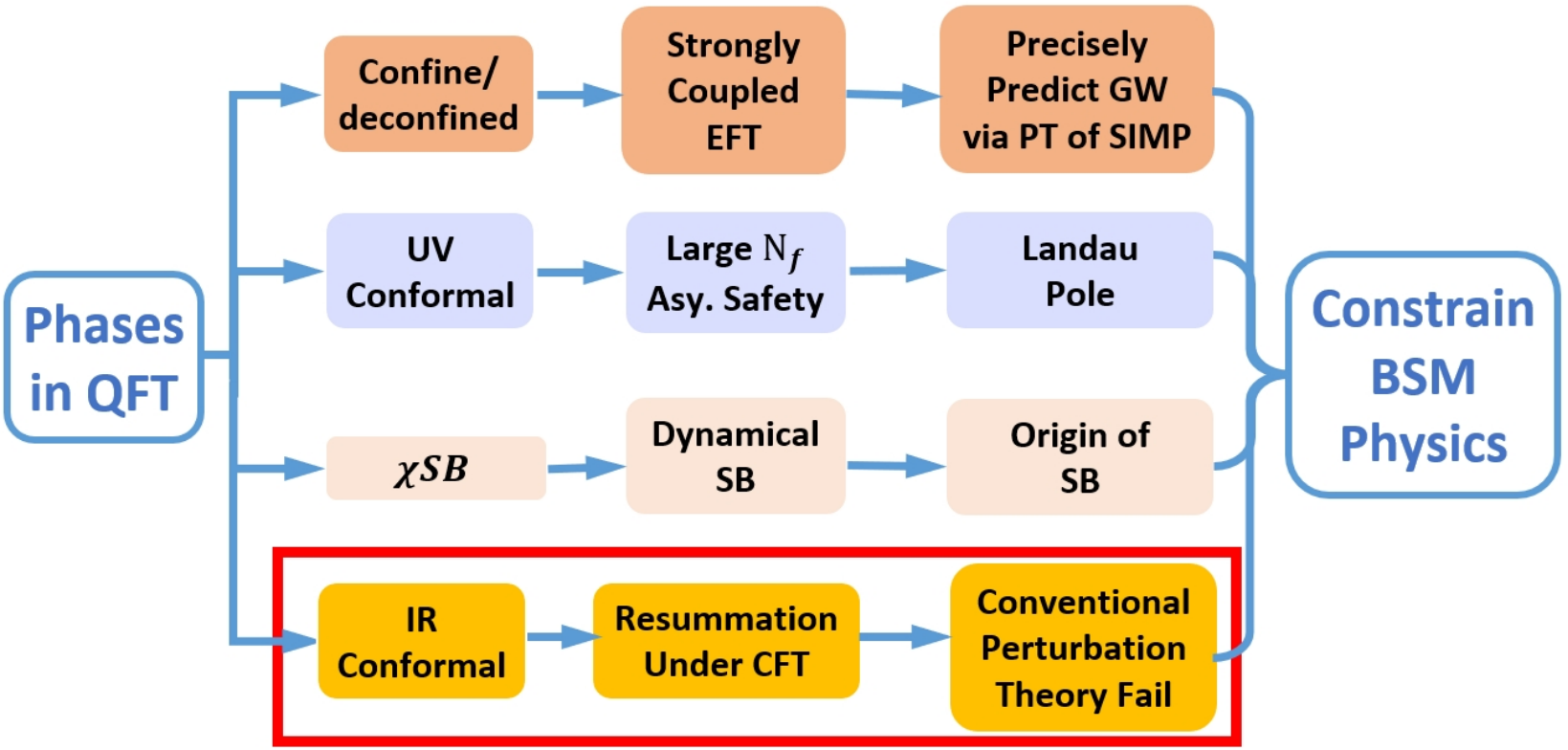

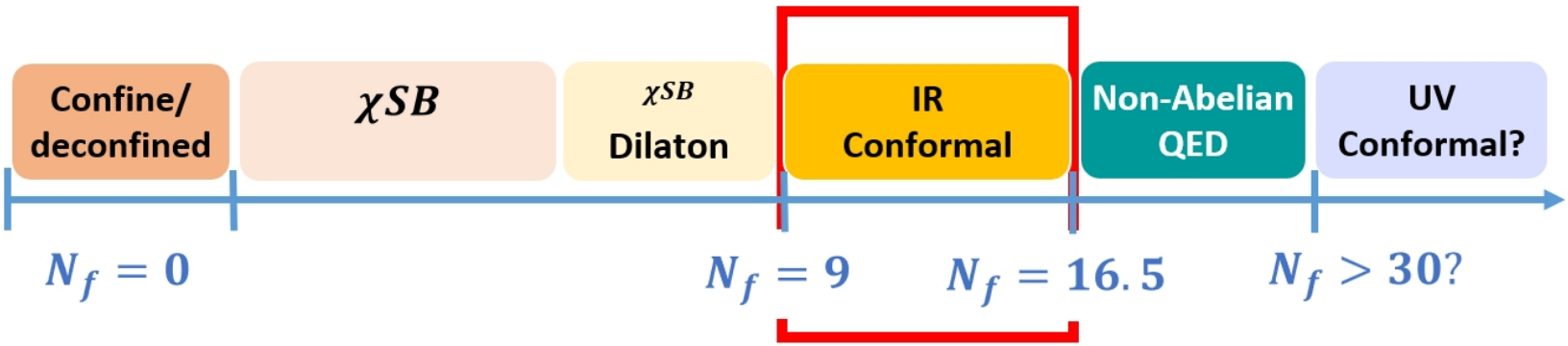

Banks-Zaks fixed point: $SU(3)$ Two-loop β-function

- The Two-loop β-function with $SU(3)$

$$\beta(g) = -\frac{\beta_0}{16\pi^2} g^3 - \frac{\beta_1}{(16\pi^2)^2} g^5 + \mathcal{O}(g^7), where$$

$$\beta_0 = \frac{11}{3} N_c - \frac{2}{3} N_f = \frac{33 - 2N_f}{3},$$

$$\beta_1 = \frac{34}{3} N_c^2 - \frac{10}{3} N_c N_f - 2\, C_F N_f = 102 - \frac{38}{3} N_f, \quad C_F = \frac{N_c^2 - 1}{2N_c} = \frac{4}{3}.$$

N_f	β_0	β_1	$\alpha_* = \frac{g_*^2}{4\pi}$
9	5	-12	5.24
10	13/3	$-74/3$	2.21
11	11/3	$-112/3$	1.23
12	3	-50	0.754
13	7/3	$-188/3$	0.468
14	5/3	$-226/3$	0.278
15	1	-88	0.143
16	1/3	$-302/3$	0.0416

IR phase: large-charge resummation

Antipin, Bersini, Sannino, Z-W W and Zhang, Phys. Rev. D 102 (2020) 045011

Antipin, Bersini, Panopoulos, Sannino, Z-W W, JHEP 02 (2024) 168

Fixed-charge sector Q, large Q double scaling with $A = \lambda Q$

IR CFT → fixed charge Q → saddle on $\mathbb{R} \times S^{d-1}$ → Δ_Q resummed

$$G_Q(\tau) \equiv \langle O_Q^\dagger(\tau) O_Q(0) \rangle_{\rm cyl} \sim e^{-\Delta_Q \tau / R},$$
$$\Delta_Q = Q F_{-1}(A) + F_0(A) + O(Q^{-1}),$$
$$A = \lambda_* Q.$$

$$\sum_\ell \lambda^\ell P_\ell(Q) \quad \Longrightarrow \quad \sum_{k \geq -1} Q^{-k} F_k(\lambda Q)$$

Large-parameter analogy

- large N_f: fixed $g^2 N_f \Rightarrow$ resummed gauge β functions.
- large Q: fixed $\lambda Q \Rightarrow$ resummed CFT dimensions Δ_Q.

Charged scalar sectors and the SM Higgs

- $O(N)$ and $U(N) \times U(M)$: LO/NLO in charge, all orders in λQ, with charge-configuration recipe.
- SM Higgs: charged-sector dimensions for $H^{I_1} \cdots H^{I_Q}$; $Q = 1$ matches known three-loop terms.
- Long goal: toward the "Holy Grail" function for multi-Higgs production.

$$\Delta_Q = Q + \left\{ \frac{1}{3}\lambda Q^2 + \left[N\mathcal{Y}_u + N\mathcal{Y}_d + \mathcal{Y}_l - \frac{3}{4}g'^2 - \frac{\lambda}{3} \right] Q \right\} - \left\{ \frac{2}{9}\lambda^2 Q^3 - \left[2N\mathcal{Y}_{uu} + 2N\mathcal{Y}_{dd} + 2\mathcal{Y}_{ll} \right.\right.$$
$$\left. - \frac{2}{3}\lambda(N\mathcal{Y}_u + N\mathcal{Y}_d + \mathcal{Y}_l) - \frac{1}{3}\lambda g'^2 + \frac{g'^4}{16} + \frac{\lambda^2}{9} \right] Q^2 + C_{22} Q \Big\} + \Big\{ \frac{8}{27}\lambda^3 Q^4 + \Big[\frac{1}{16} g'^6 (9\zeta(3) - 1)$$
$$- \frac{1}{6} g'^4 \lambda (1 + 3\zeta(3)) + \frac{1}{3} g'^2 \lambda^2 (3 - 2\zeta(3)) + \frac{4}{27}\lambda^3 (9\zeta(3) - 8) + \frac{4}{27} \big(3N \left(\lambda^2 \mathcal{Y}_u - 3\lambda \mathcal{Y}_{uu} \right.$$
$$+ 9\zeta(3)(\lambda \mathcal{Y}_{uu} - 2\mathcal{Y}_{uuu})) + 3N \left(\lambda^2 \mathcal{Y}_d - 3\lambda \mathcal{Y}_{dd} + 9\zeta(3)(\lambda \mathcal{Y}_{dd} - 2\mathcal{Y}_{ddd}) \right) + 3 \left(\lambda^2 \mathcal{Y}_l - 3\lambda \mathcal{Y}_{ll} \right.$$
$$\left. \left. + 9\zeta(3)(\lambda \mathcal{Y}_{ll} - 2\mathcal{Y}_{lll}) \right) \big) \Big] Q^3 + C_{23} Q^2 + C_{33} Q \Big\} + \mathcal{O}\left(\kappa_I^4 Q^5 \right) . \qquad (7.1)$$

where red, blue, and orange colors highlight the terms stemming from the small $\kappa_I Q$ expansion of Δ_{-1}, $\Delta_0^{\rm fm}$, and $\Delta_0^{\rm bos}$.

IR phase: Banks-Zaks or Coleman-Weinberg

Hansen, Janowski, Langæble, Mann, Sannino, Steele, Z-W W, Phys. Rev. D 97 (2018) 065014.

CAF $SU(N_c)$ model

$$\mathcal{L} = -\frac{1}{2}\,\mathrm{Tr}F_{\mu\nu}^2 + \overline{Q}\,\not{D}Q + \mathrm{Tr}(D_\mu S^\dagger D^\mu S) - v(\,\mathrm{Tr}S^\dagger S)^2 - u\,\mathrm{Tr}(S^\dagger S)^2.$$

$SU(N_c)$ + N_f quarks + N_s scalar quarks

UV: $\alpha, \lambda_1, \lambda_2 \to 0$, $\quad \lambda_i/\alpha =$ fixed flow.

One UV boundary, two IR fates

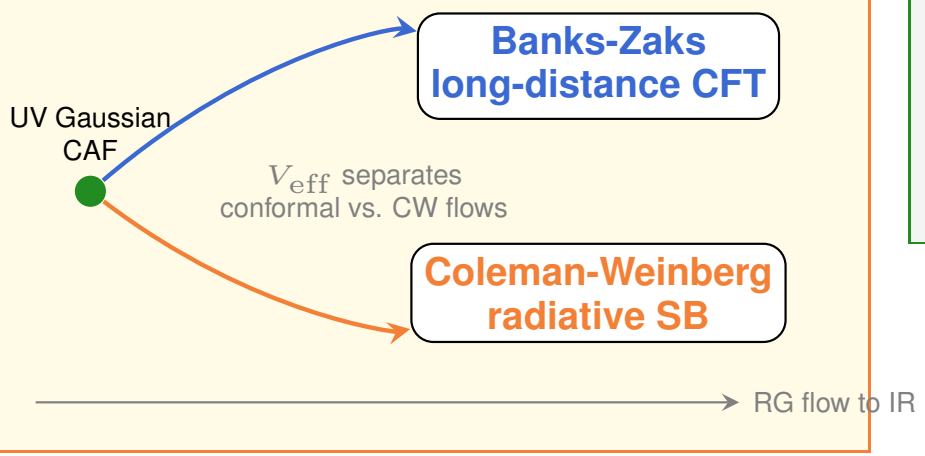

UV free → IR structure

- Perturbative phase diagram of completely asymptotically free gauge theories with fermions and scalar quarks.
- CAF fixes the UV Gaussian boundary and allowed fixed-flow trajectories for $\alpha, \lambda_1, \lambda_2$.
- Gauge Banks-Zaks fixed point plus scalar fixed points give long-distance conformality.
- Quantum-corrected Coleman-Weinberg/Gildener-Weinberg potential separates conformal flows from radiative symmetry breaking.

$$\beta_\alpha = -B\alpha^2 + C\alpha^3 + \cdots, \qquad \alpha_*^{\rm BZ} = B/C.$$

UV free → IR BZ CFT

or IR CW breaking

Confine/Deconfined Phase

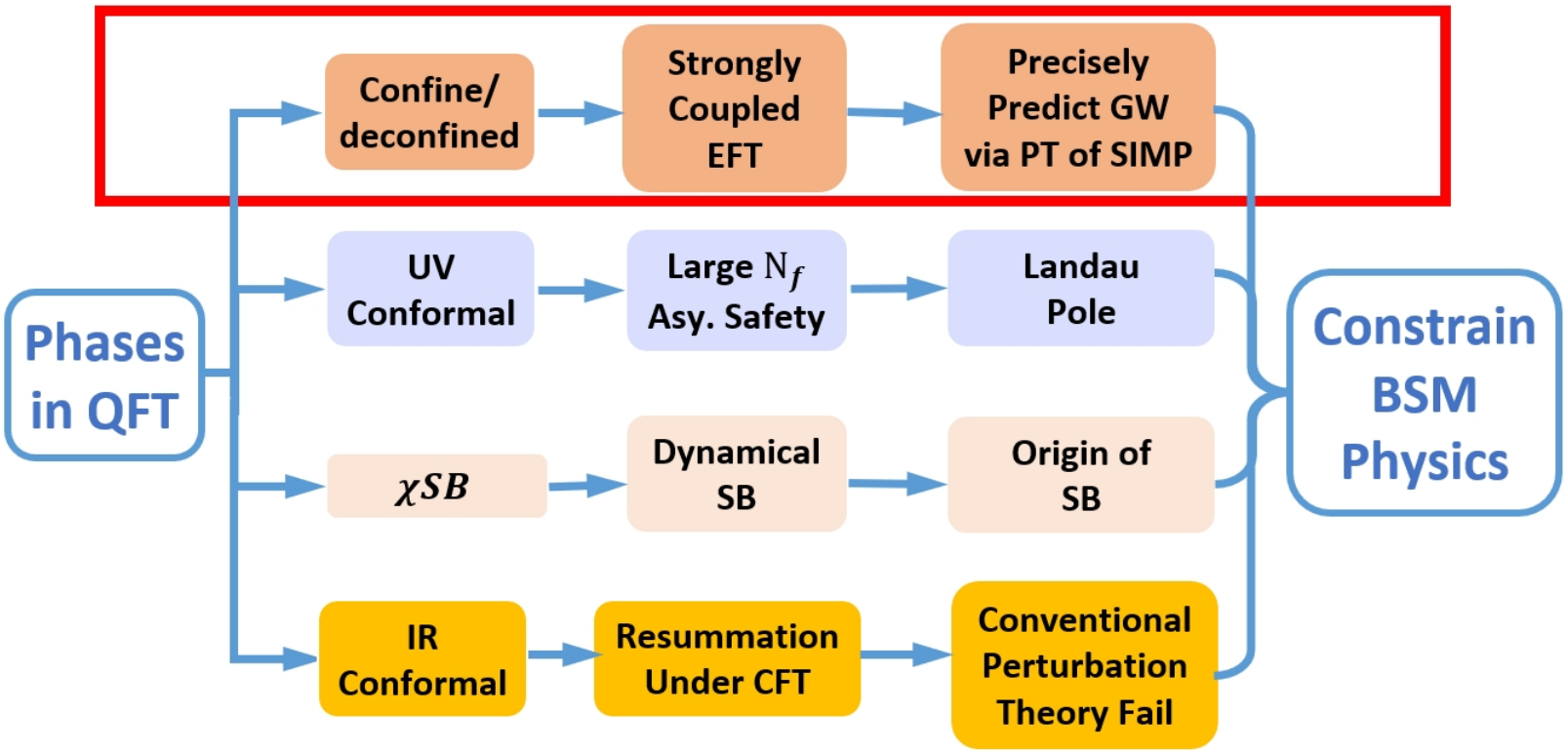

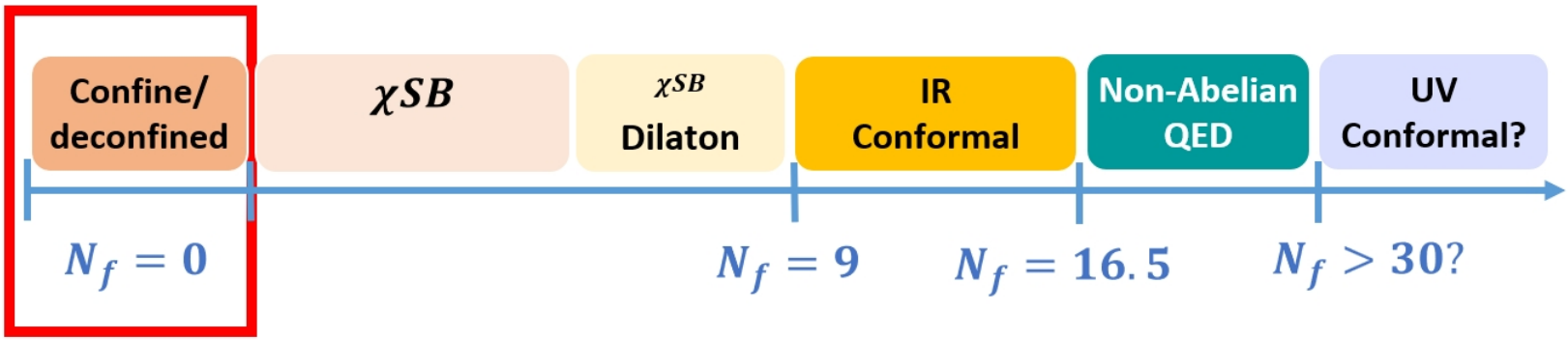

Outline: From Phase Transition Dynamics to Detection

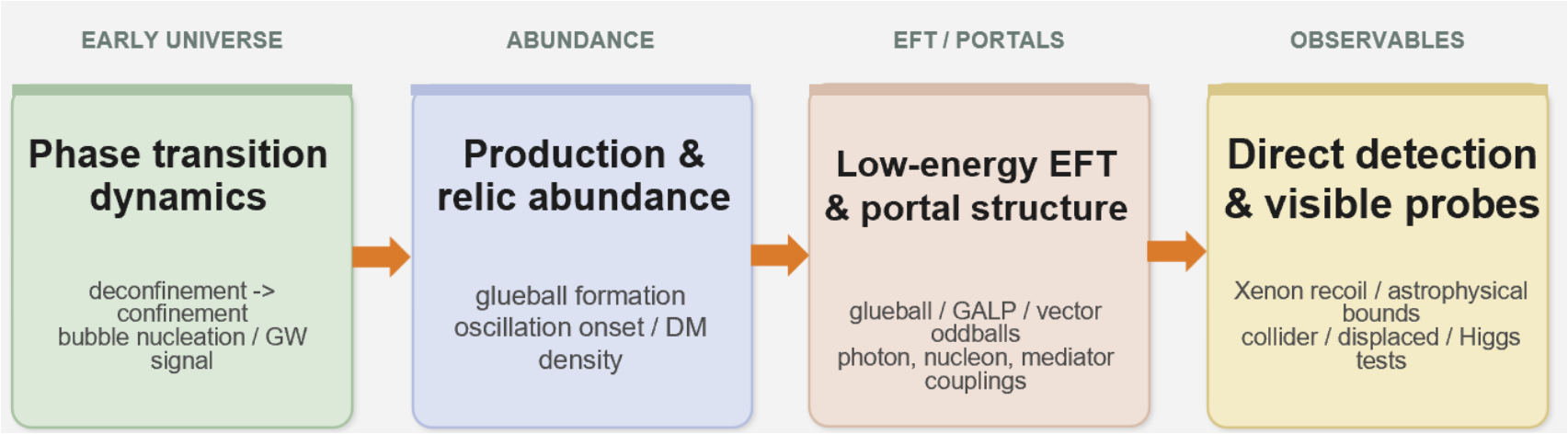

Dark confinement first sets the transition dynamics, then the relic abundance, and finally the portal structure tested by direct detection and collider searches.

What composes the strongly coupled sector?

- Dark Yang-Mills theories
- Pure gluons $\Rightarrow$ confinement-deconfinement phase transition
- Gluons + Fermions
  - Fermions in fundamental representation $\Rightarrow$ chiral phase transition
  - Fermions in adjoint rep. $\Rightarrow$ confinement & chiral phase transition
  - Fermions in 2-index symmetric rep. $\Rightarrow$ confinement & chiral phase transition
- Gluons + Fermions + Scalars (not explored yet)

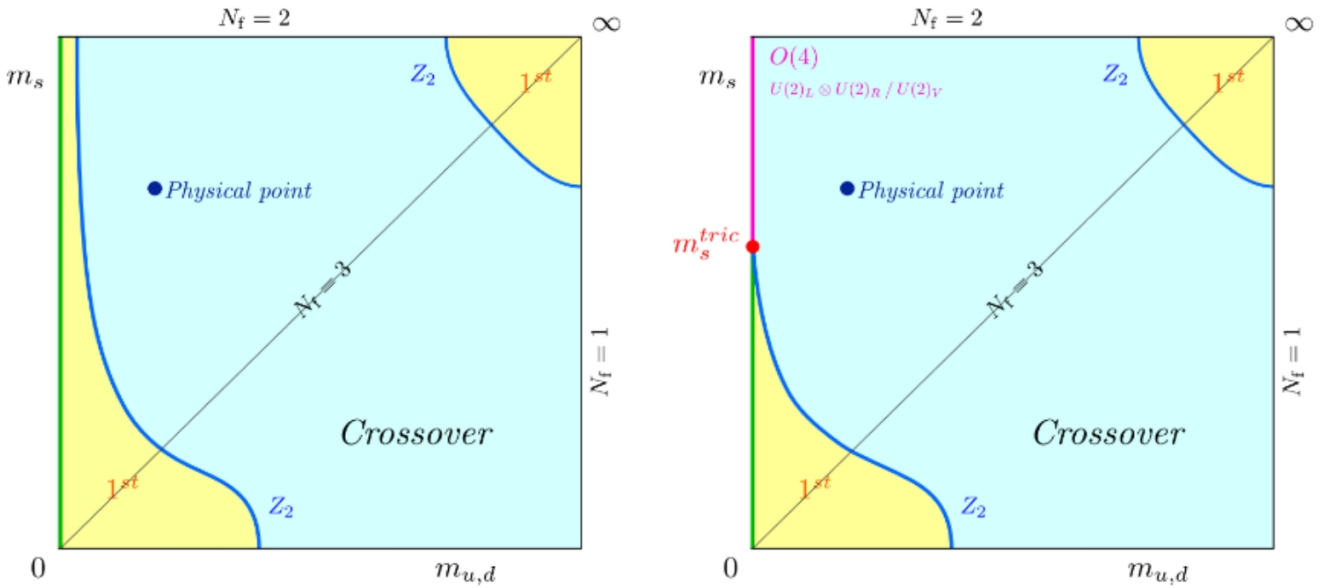

图: Finite-T Columbia plot: for $m_{u,d} = 0$, the $N_f = 2$ chiral transition is first order below m_s^{tric} and second order above it; the latter may belong to the $O(4)$ or $U(2)_L \times U(2)_R/U(2)_V$ universality class, depending on effective $U(1)_A$ restoration near T_c.

How to describe the strongly coupled sector?

- Pure gluons
  - Polyakov loop model (Huang, Reichert, Sannino and Z-W W, PRD **104** (2021) 035005; Kang, Zhu, Matsuzaki, JHEP 09 (2021) 060; Gao, Sun and White, arXiv:2405.00490.)
  - Matrix Model (Halverson, Long, Maiti, Nelson, Salinas, JHEP **05** (2021) 154)
  - Holographic QCD model (Ares, Henriksson, Hindmarsh, Hoyos, Jokela, PRD **105** (2022) 066020; Ares, Henriksson, Hindmarsh, Hoyos, Jokela, PRL **128** (2022) 131101)
- Gluons + Fermions
  - Polyakov loop improved Nambu-Jona-Lasinio model (Reichert, Sannino, Z-W W and Zhang, JHEP **01** (2022) 003; Helmboldt, Kubo, Woude, PRD **100** (2019) 055025)
  - Linear sigma model (Helmboldt, Kubo, Woude, PRD **100** (2019) 055025)
  - Polyakov Quark Meson model (Pasechnik, Reichert, Sannino, Z-W W, JHEP **02** (2024) 159)

Procedure of pure gluon case

(Huang, Reichert, Sannino and Z-W W, PRD **104** (2021) 035005

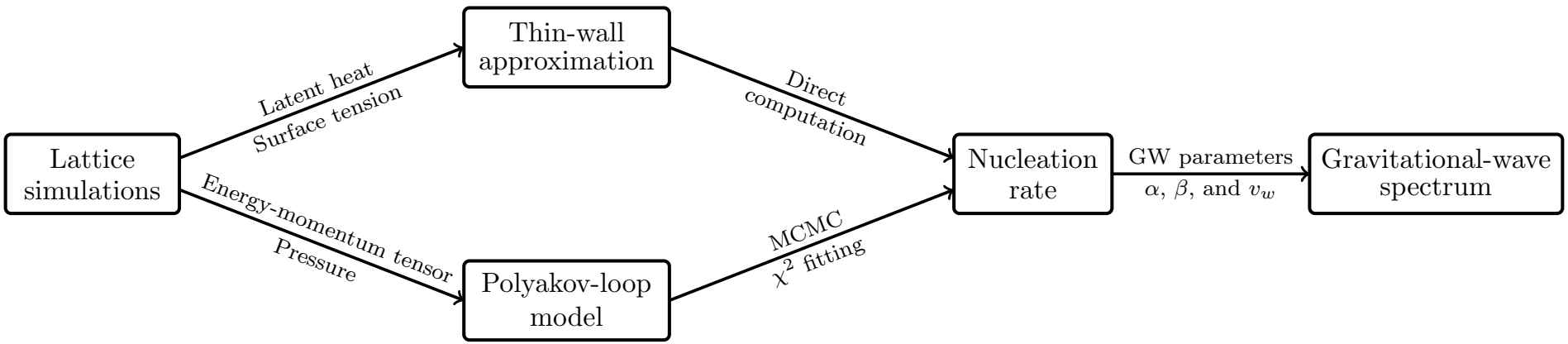

Polyakov Loop Model

Polyakov Loop Model for Pure Gluons: I

- Pisarski first proposed the Polyakov-loop Model as an effective field theory to describe the confinement-deconfinement phase transition of $SU(N)$ gauge theory (Pisarski, PRD **62** (2000) 111501).
- In a local $SU(N)$ gauge theory, a global center symmetry $Z(N)$ is used to distinguish confinement phase (unbroken phase) and deconfinement phase (broken phase)
- An order parameter for the $Z(N)$ symmetry is constructed using the Polyakov Loop (thermal Wilson line) (Polyakov, PLB 72 (1978) 477)

$$\mathbf{L}(\vec{x}) = \mathcal{P} \exp\left[i \int_0^{1/T} A_4(\vec{x}, \tau)\, \mathrm{d}\tau \right]$$

The symbol $\mathcal{P}$ denotes path ordering and A_4 is the Euclidean temporal component of the gauge field

- The Polyakov Loop transforms like an adjoint field under local $SU(N)$ gauge transformations

Polyakov Loop Model for Pure Gluons: II

- Convenient to define the trace of the Polyakov loop as an order parameter for the $Z(N)$ symmetry

$$\ell\left(\vec{x}\right) = \frac{1}{N}\mathrm{Tr}_c[\mathbf{L}]\,,$$

where Tr_c denotes the trace in the colour space.

- Under a global $Z(N)$ transformation, the Polyakov loop ℓ transforms as a field with charge one

$$\ell \to e^{i\phi}\ell, \qquad \phi = \frac{2\pi j}{N}, \qquad j = 0, 1, \cdots, (N-1)$$

- The expectation value of ℓ i.e. $<\ell>$ has the important property:

$$\langle\ell\rangle = 0 \quad (T < T_c, \text{ Confined})\,; \qquad \langle\ell\rangle > 0 \quad (T > T_c, \text{ Deconfined})$$

- At very high temperature, the vacua exhibit a $N-$fold degeneracy:

$$\langle\ell\rangle = \exp\left(i\frac{2\pi j}{N}\right)\ell_0, \qquad j = 0, 1, \cdots, (N-1)$$

where ℓ_0 is defined to be real and $\ell_0 \to 1$ as $T \to \infty$

Polyakov loop $\Rightarrow$ static-quark free energy?

Physical picture

At finite temperature, Euclidean time is not an infinite line, but a circle of length $\beta = \frac{1}{T}$.
Now insert one **infinitely heavy, static** fundamental quark. Since it is static, it does not move in space. It only propagates from $\tau = 0$ to $\tau = \beta$, namely, it wraps once around the thermal circle.
The color phase accumulated along this worldline is precisely the **Polyakov loop**.

Translation into free energy

Define the free-energy cost of inserting one static quark by

$$F_Q^{\mathrm{bare}} \equiv -T \ln \frac{Z_Q}{Z}.$$

After removing the trivial heavy-mass term M and the UV self-energy of the static color source, one obtains the **renormalized** relation

$$F_Q = -T \ln \langle \ell \rangle_{\mathrm{ren}}, \qquad \boxed{\langle \ell \rangle_{\mathrm{ren}} = e^{-F_Q/T}}.$$

One-sentence summary: The Polyakov loop is the amplitude for a static quark to go once around the thermal circle, and in the thermal ensemble this amplitude is exactly the Boltzmann factor associated with the free-energy cost of inserting that source.

Strictly speaking, the bare Polyakov loop contains the divergent self-energy of the static color source, so the final physical relation should be written in terms of the renormalized quantity $\langle \ell \rangle_{\mathrm{ren}}$.

Summary of Pure Gluon Facts

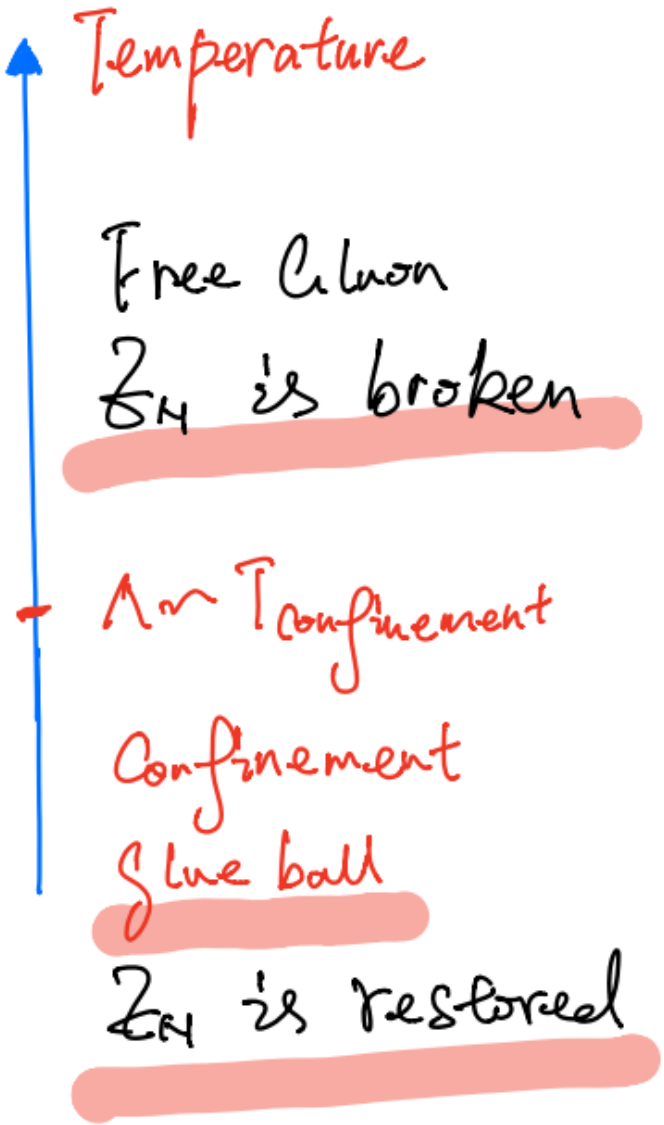

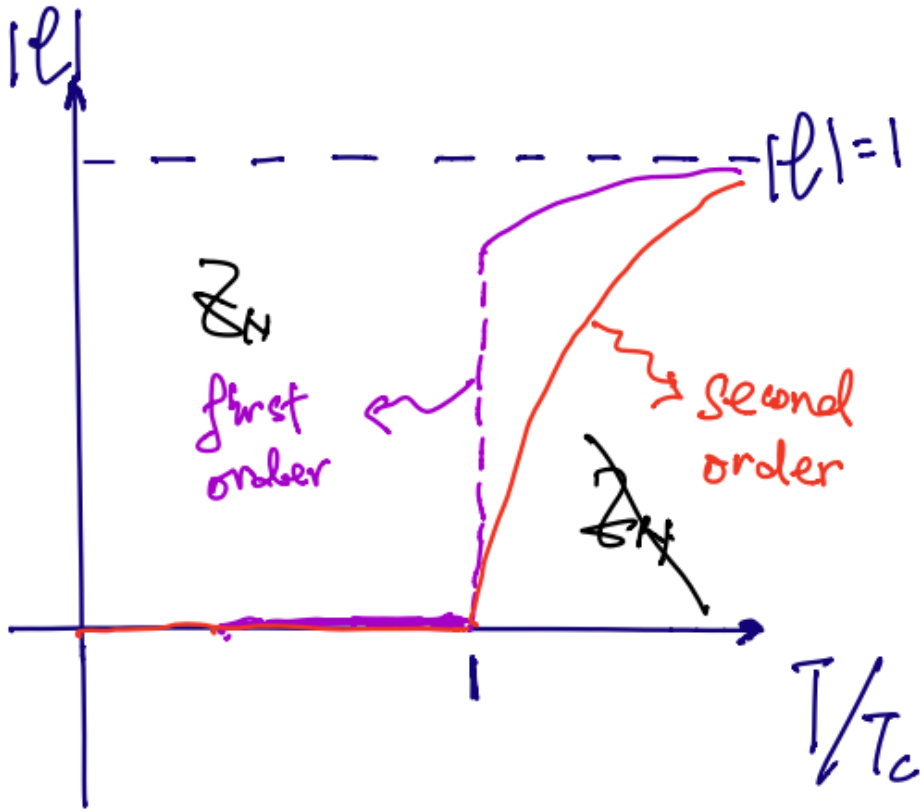

Second Order for SU(2)

First order SU(N) (N≥3)

Effective Potential of the Polyakov Loop Model: I

- The simplest effective potential preserving the Z_N symmetry in the polynomial form is given by (Pisarski, PRD **62** (2000) 111501)

$$V_{\rm PLM}^{(\rm poly)} = T^4\left(-\frac{b_2(T)}{2}|\ell|^2 + b_4|\ell|^4 + \cdots - b_3\left(\ell^N + \ell^{*N}\right)\right)$$

$$\text{where}\quad b_2(T) = a_0 + a_1\left(\frac{T_0}{T}\right) + a_2\left(\frac{T_0}{T}\right)^2 + a_3\left(\frac{T_0}{T}\right)^3 + a_4\left(\frac{T_0}{T}\right)^4$$

"$\cdots$" represent any required lower dimension operator than ℓ^N i.e. $(\ell\ell^*)^k = |\ell|^{2k}$ with $2k < N$.

- For the $SU(3)$ case, there is also an alternative logarithmic form

$$V_{\rm PLM}^{(\rm 3log)} = T^4\left(-\frac{a(T)}{2}|\ell|^2 + b(T)\ln\left(1 - 6|\ell|^2 + 4(\ell^{*3} + \ell^3) - 3|\ell|^4\right)\right)$$

$$a(T) = a_0 + a_1\left(\frac{T_0}{T}\right) + a_2\left(\frac{T_0}{T}\right)^2 + a_3\left(\frac{T_0}{T}\right)^3, \quad b(T) = b_3\left(\frac{T_0}{T}\right)^3$$

- The a_i, b_i coefficients in $V_{\rm PLM}^{(\rm poly)}$ and $V_{\rm PLM}^{(\rm 3log)}$ are determined by fitting the lattice results

Fitting the Coefficients Using the Lattice Results: I

Marco Panero, Phys.Rev.Lett. 103 (2009) 232001

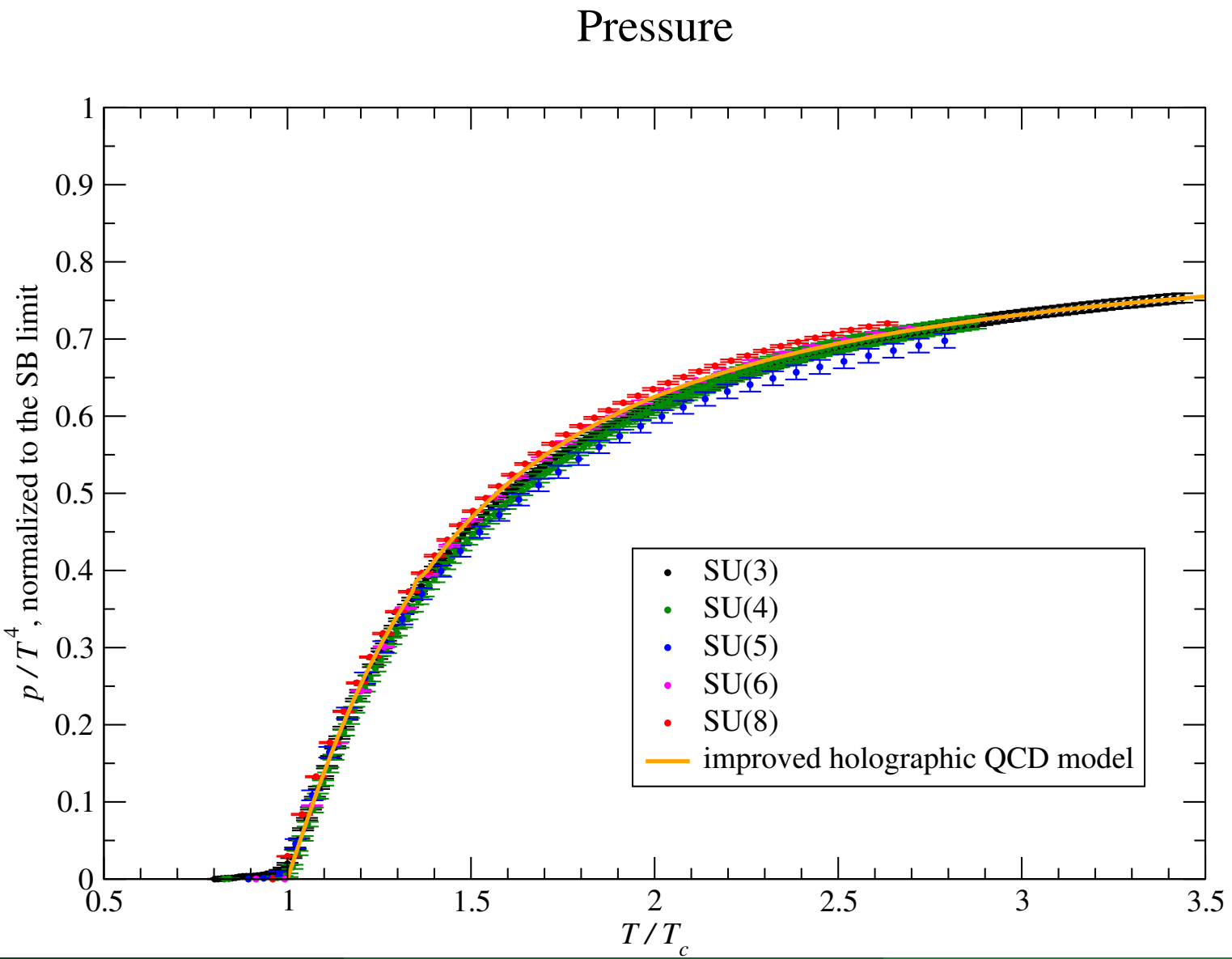

Fitting the Coefficients Using the Lattice Results: II

Marco Panero, Phys.Rev.Lett. 103 (2009) 232001

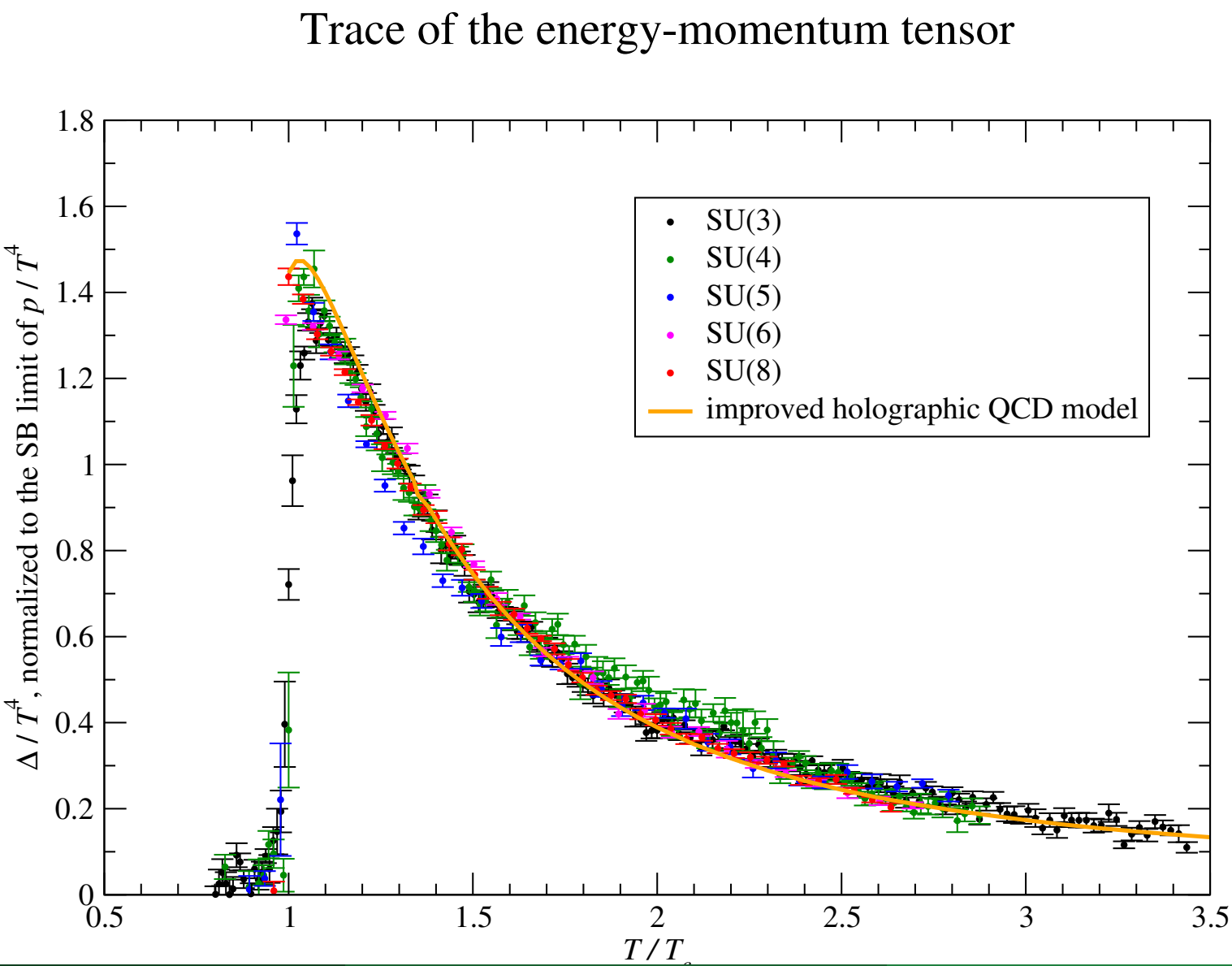

Fitting the Coefficients Using the Lattice Results: III

(Huang, Reichert, Sannino and Z-W W, PRD **104** (2021) 035005

Fitted to lattice data of pressure and the trace of energy momentum tensor.

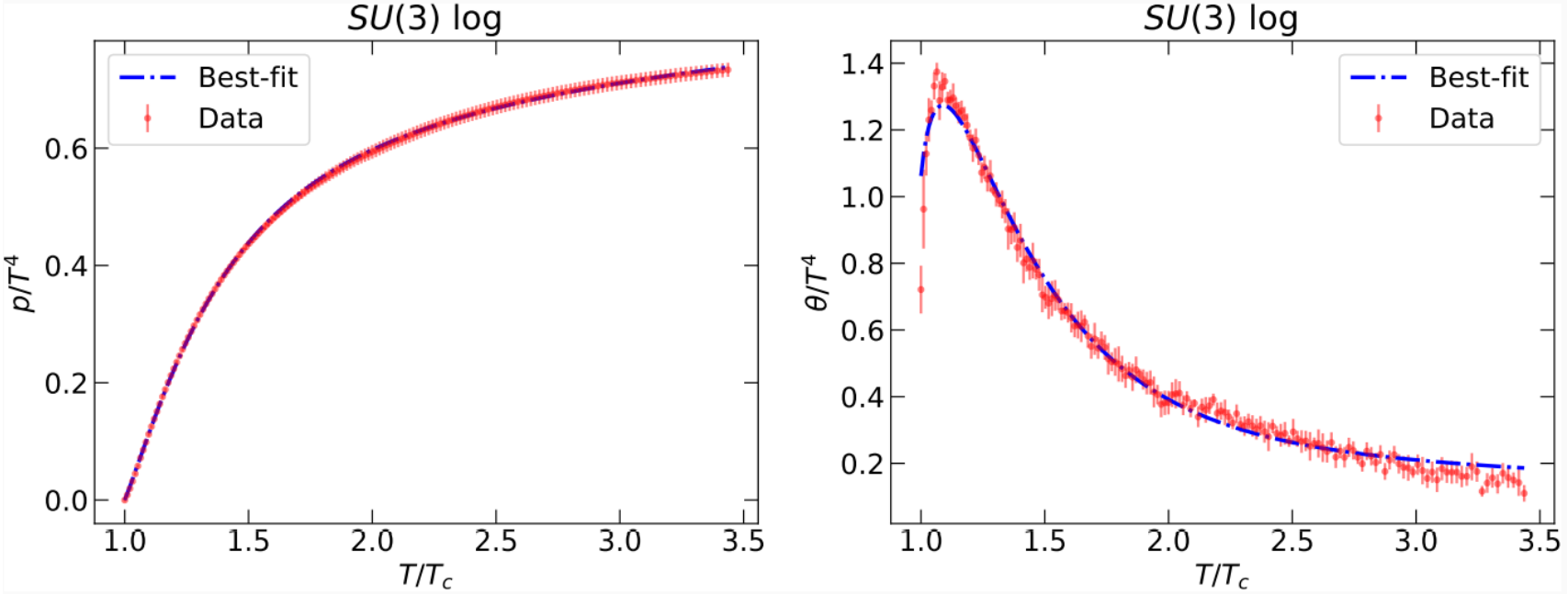

Include Fermions：the PNJL Model and PQM Model

K. Fukushima, PLB **591** (2004) 277; Ratti, Thaler Weise, PRD **73** (2006) 014019
B. Schaefer, J. Pawlowski, J. Wambach PRD **76** (2007) 074023; B. Schaefer, M. Wagner, PPNP **62** (2009) 391
Reichert, Sannino, Z-W W and Zhang, JHEP **01** (2022) 003, arXiv:2109.11552.
Pasechnik, Reichert, Sannino and Z-W W,JHEP **02** (2024) 159.

- The Polyakov-loop-Nambu-Jona-Lasinio (PNJL) model is used to describe phase-transition dynamics in dark gauge-fermion sectors
- The finite-temperature grand potential of the PNJL models can be generically written as

$$V_{\mathrm{PNJL}} = V_{\mathrm{PLM}}[\ell, \ell^*] + V_{\mathrm{cond}}\left[\langle\bar{\psi}\psi\rangle\right] + V_{\mathrm{zero}}\left[\langle\bar{\psi}\psi\rangle\right] + V_{\mathrm{medium}}\left[\langle\bar{\psi}\psi\rangle, \ell, \ell^*\right]$$

- The Polyakov quark meson model (PQM) is widely used as an effective theory to study the first order chiral phase transition
- The Lagrangian of the PQM where mesons couple to a spatially constant temporal background gauge field reads

$$\mathcal{L} = \bar{q}\left(i\not{D} - g\left(\sigma + i\gamma_5 T^a \pi_a\right)\right) q + \frac{1}{2}\left(\partial_\mu \sigma\right)^2 + \frac{1}{2}\left(\partial_\mu \pi_a\right)^2$$
$$- V_{\mathrm{PLM}}^{(\mathrm{poly})} + V_{\mathrm{LSM}} + V_{\mathrm{medium}}\,, \text{where } \not{D} = \gamma_\mu \partial_\mu - i\gamma_0 A_0$$

- The finite temperature contributions to the potential of linear sigma model are typically via CJT resummation.

Second Part: Bubble Nucleation and Gravitatioanl Wave

Bubble Profile of Confinement Phase Transition

(Huang, Reichert, Sannino and Z-W W, PRD **104** (2021) 035005

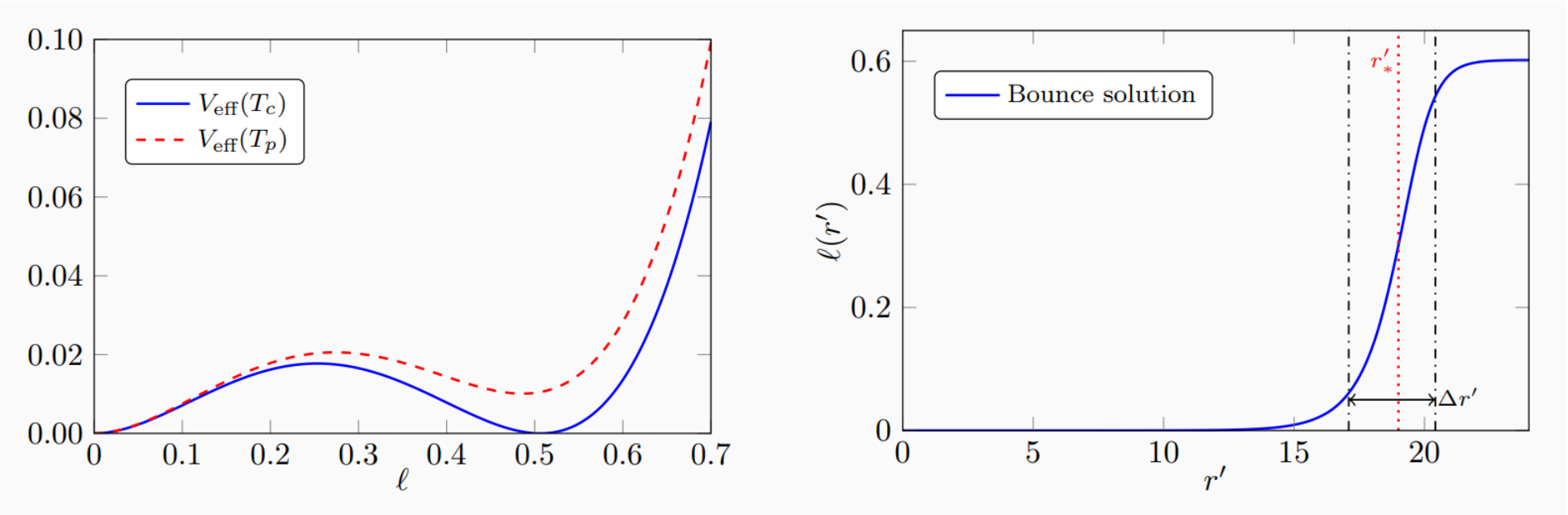

图: The bubble radius is indicated by r'_* and the wall width by $\Delta r'$. Inside of the bubble ($r' \ll r'_*$) lying the confinement phase, the Z_N symmetry is unbroken and $\langle \ell \rangle = 0$, while outside of the bubble ($r \gg r'_*$) lying the deconfinement phase, the Z_N symmetry is broken and $\langle \ell \rangle > 0$.

Gravitational-wave spectrum

(Huang, Reichert, Sannino and Z-W W, PRD **104** (2021) 035005)

- Contributions from bubble collision and turbulence are subleading
- The GW spectrum from sound waves is given by

$$h^2\Omega_{\rm GW}(f) = h^2\Omega_{\rm GW}^{\rm peak}\left(\frac{f}{f_{\rm peak}}\right)^3\left[\frac{4}{7}+\frac{3}{7}\left(\frac{f}{f_{\rm peak}}\right)^2\right]^{-\frac{7}{2}}$$

- The peak frequency

$$f_{\rm peak} \simeq 1.9\cdot 10^{-5}\,{\rm Hz}\left(\frac{g_*}{100}\right)^{\frac{1}{6}}\left(\frac{T}{100\,{\rm GeV}}\right)\left(\frac{\tilde{\beta}}{v_w}\right)$$

- The peak amplitude

$$h^2\Omega_{\rm GW}^{\rm peak} \simeq 2.65\cdot 10^{-6}\left(\frac{v_w}{\tilde{\beta}}\right)\left(\frac{\kappa_{sw}\,\alpha}{1+\alpha}\right)^2\left(\frac{100}{g_*}\right)^{\frac{1}{3}}\Omega_{\rm dark}^2$$

- The factor $\Omega_{\rm dark}^2$ accounts for the dilution of the GWs by the non-participating SM d.o.f.

$$\Omega_{\rm dark} = \frac{\rho_{\rm rad,dark}}{\rho_{\rm rad,tot}} = \frac{g_{*,\rm dark}}{g_{*,\rm dark}+g_{*,\rm SM}}$$

The Efficiency Factor κ

- The efficiency factor for the sound waves $\kappa_{\rm sw}$ consist of κ_v as well as an additional suppression due to the length of the sound-wave period $\tau_{\rm sw}$

$$\kappa_{\rm sw} = \sqrt{\tau_{\rm sw}}\,\kappa_v$$

- $\tau_{\rm sw}$ is dimensionless and measured in units of the Hubble time (H.-K. Guo, Sinha, Vagie and White, JCAP **01** (2021) 001)

$$\tau_{\rm sw} = 1 - 1/\sqrt{1 + 2\frac{(8\pi)^{\frac{1}{3}} v_w}{\tilde{\beta}\,\bar{U}_f}} \Rightarrow \tau_{\rm sw} \sim \frac{(8\pi)^{\frac{1}{3}} v_w}{\tilde{\beta}\,\bar{U}_f} \ \text{for}\ \beta >> 1$$

where $\bar{U}_f$ is the root-mean-square fluid velocity

$$\bar{U}_f^2 = \frac{3}{v_w(1+\alpha)} \int_{c_s}^{v_w} \mathrm{d}\xi\, \xi^2 \frac{v(\xi)^2}{1 - v(\xi)^2} \simeq \frac{3}{4}\frac{\alpha}{1+\alpha}\kappa_v$$

- $\tau_{\rm sw}$ is suppressed for large β occurring often in strongly coupled sectors
- κ_v was numerically fitted to simulation results depends α and v_w. At the Chapman-Jouguet detonation velocity it reads

$$\kappa_v(v_w = v_J) = \frac{\sqrt{\alpha}}{0.135 + \sqrt{0.98 + \alpha}}$$

GW Signatures for Arbitrary N in the Pure Gluon Case

(Huang, Reichert, Sannino and Z-W W, PRD **104** (2021) 035005)

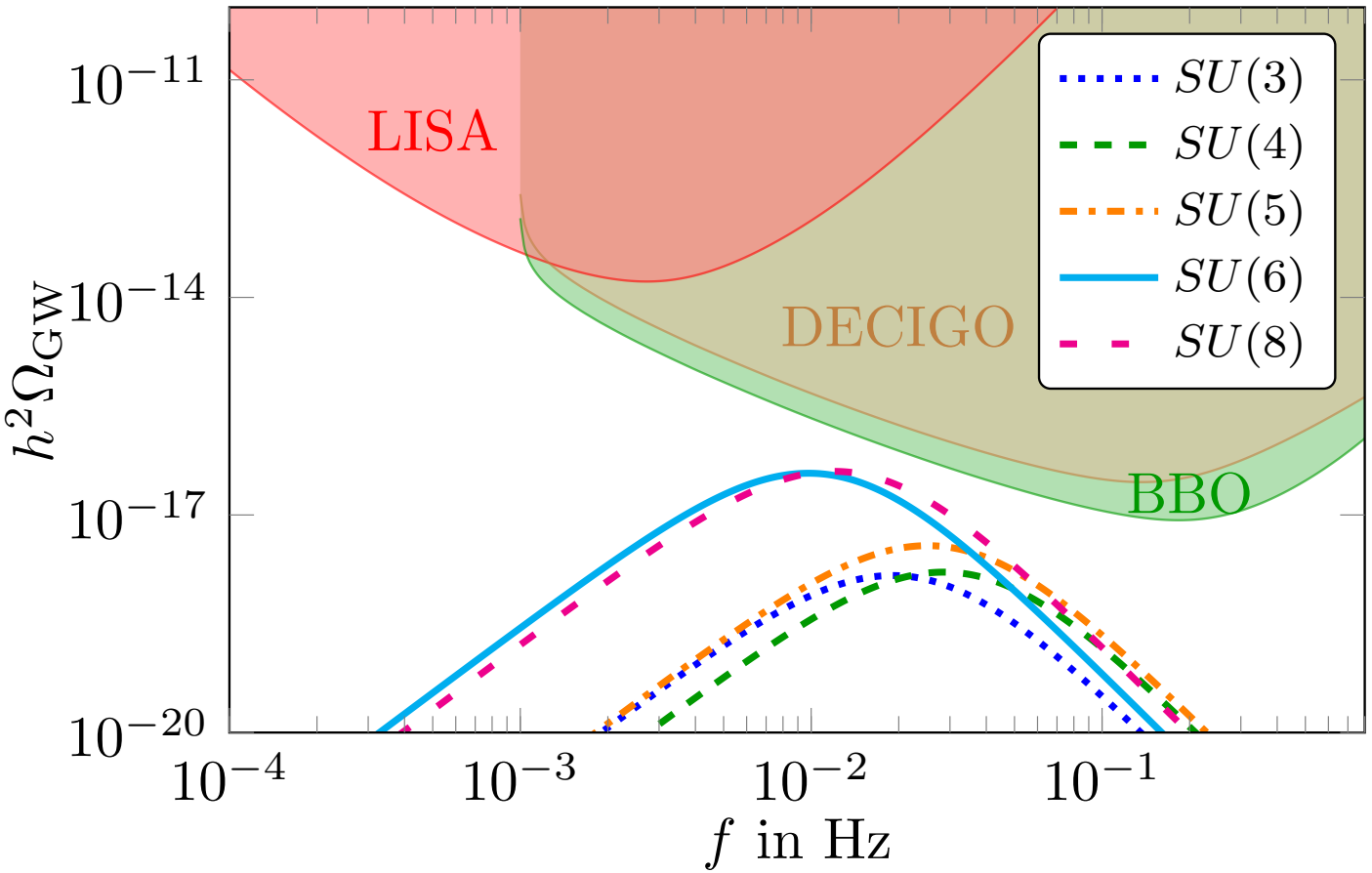

图: The dependence of the GW spectrum on the number of dark colours is shown for the values $N = 3, 4, 5, 6, 8$. All spectra are plotted with the bubble wall velocity set to the Chapman-Jouguet detonation velocity and with Tc$= 1\,\mathrm{GeV}$.

A Landscape of GW Signatures with Pure Gluon

(Huang, Reichert, Sannino and Z-W W, PRD **104** (2021) 035005)

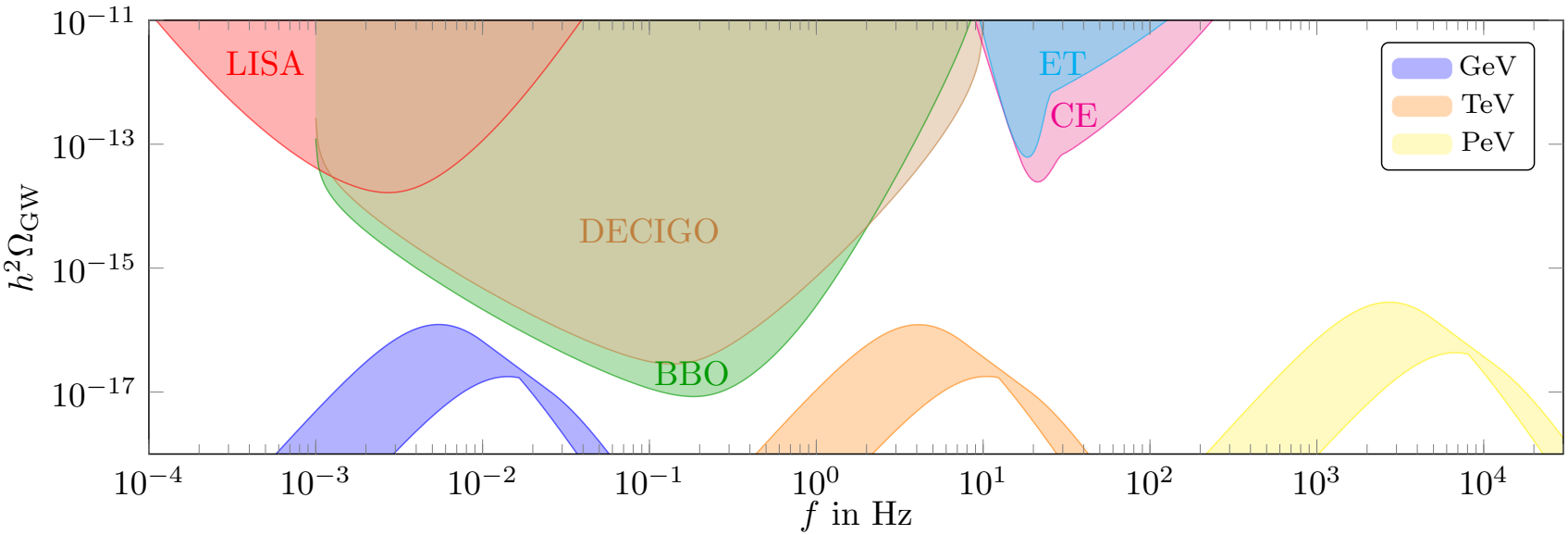

图: We display the GW spectrum of the $SU(6)$ phase transition for different confinement scales including $T_c = 1$ GeV, 1 TeV, and 1 PeV. We compare it to the power-law integrated sensitivity curves of LISA, BBO, DECIGO, CE, and ET.

Landscape of GW spectrum with three Dirac fermions

(Reichert, Sannino, Z-W W and Zhang, JHEP **01** (2022) 003, arXiv:2109.11552.)

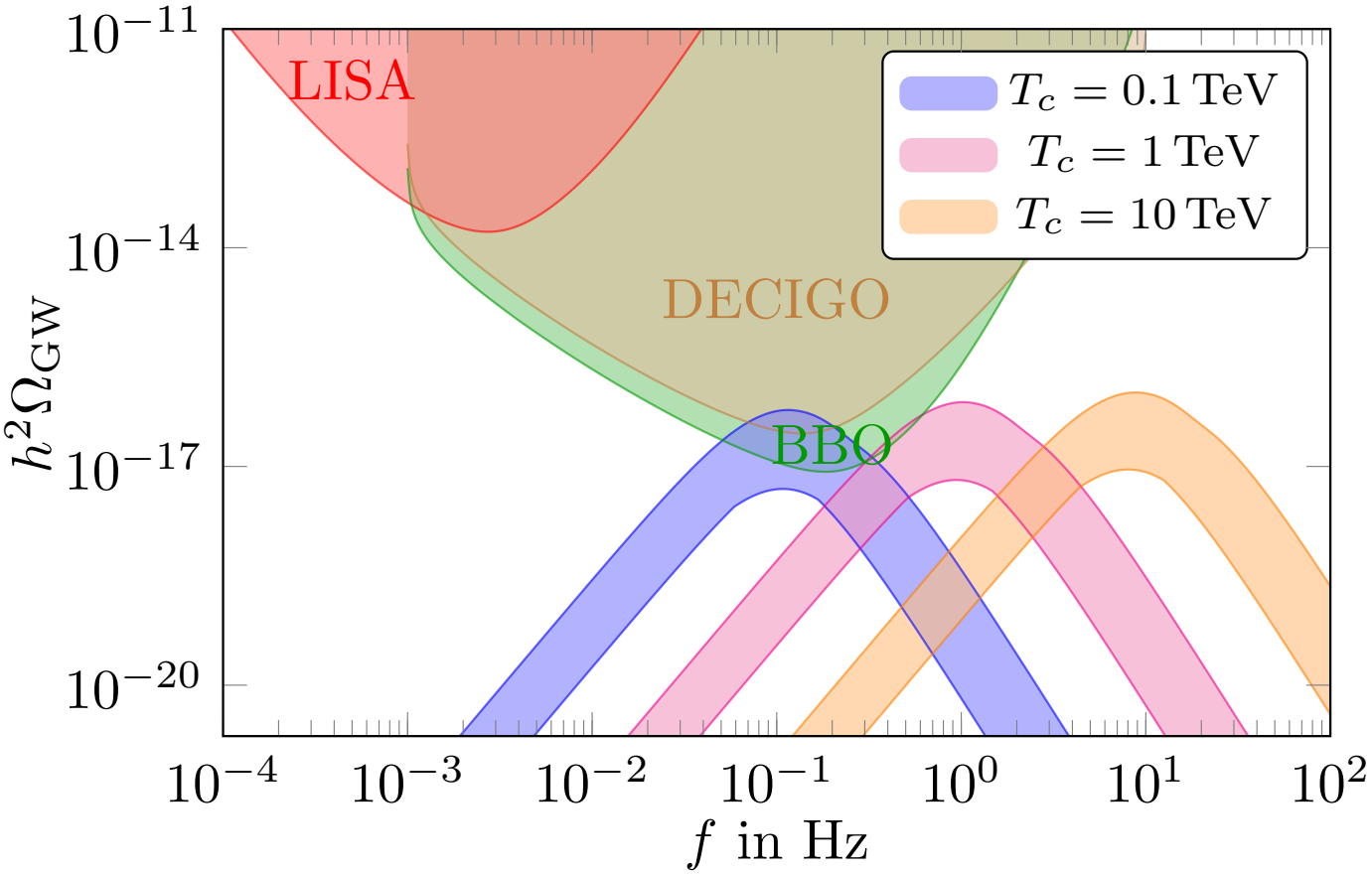

图: Gravitational-wave spectrum with three Dirac fermions in the fundamental representation for different critical temperatures. The band comes from varying wall velocity $c_s \leq v_w \leq 1$.

$\alpha - \beta$ Phase diagram via PQM Model

(Pasechnik, Reichert, Sannino and Z-W W, JHEP **02** (2024) 159.)

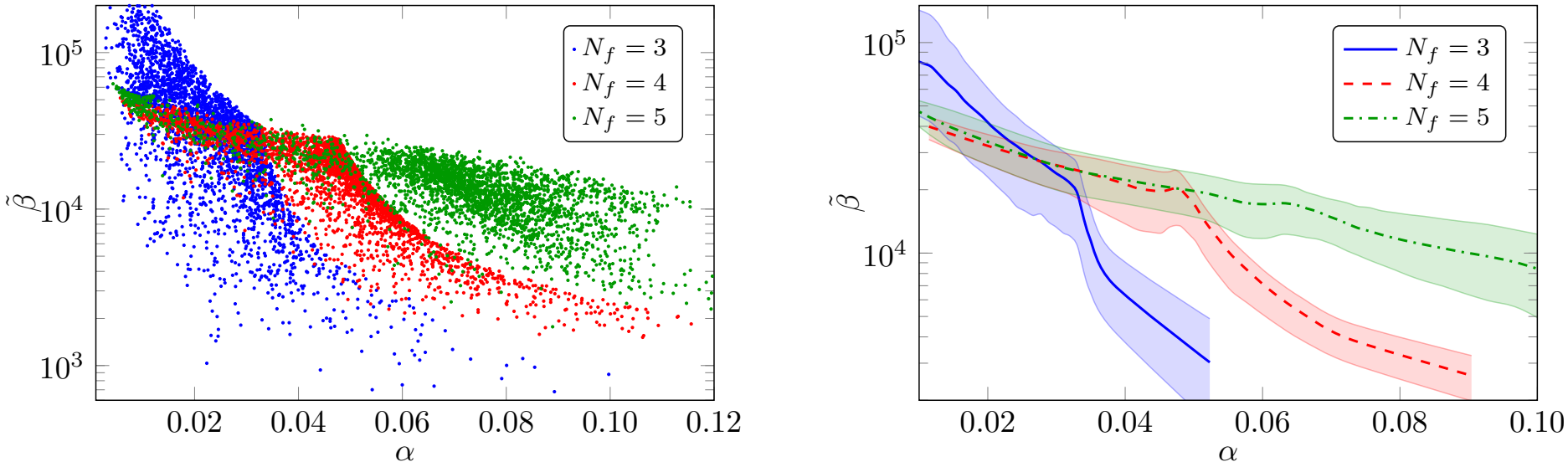

图: We show the range of α and $\tilde{\beta}$ values of the LSM for $N_f = 3, 4, 5$. In the left panel, we show the actual distribution of theory points, while in the right panel, we display the averaged values. On average, the LSM produces stronger GW signals with increasing N_f due to the larger α values. Nonetheless, the strongest GW signals are achieved with the LSM for $N_f = 3$, corresponding to the sparse blue dots at small $\tilde{\beta}$ in the left panel.

Strongest GW Signal at Small $m_\sigma \to$ Near Conformal

(Pasechnik, Reichert, Sannino and Z-W W, JHEP **02** (2024) 159.)

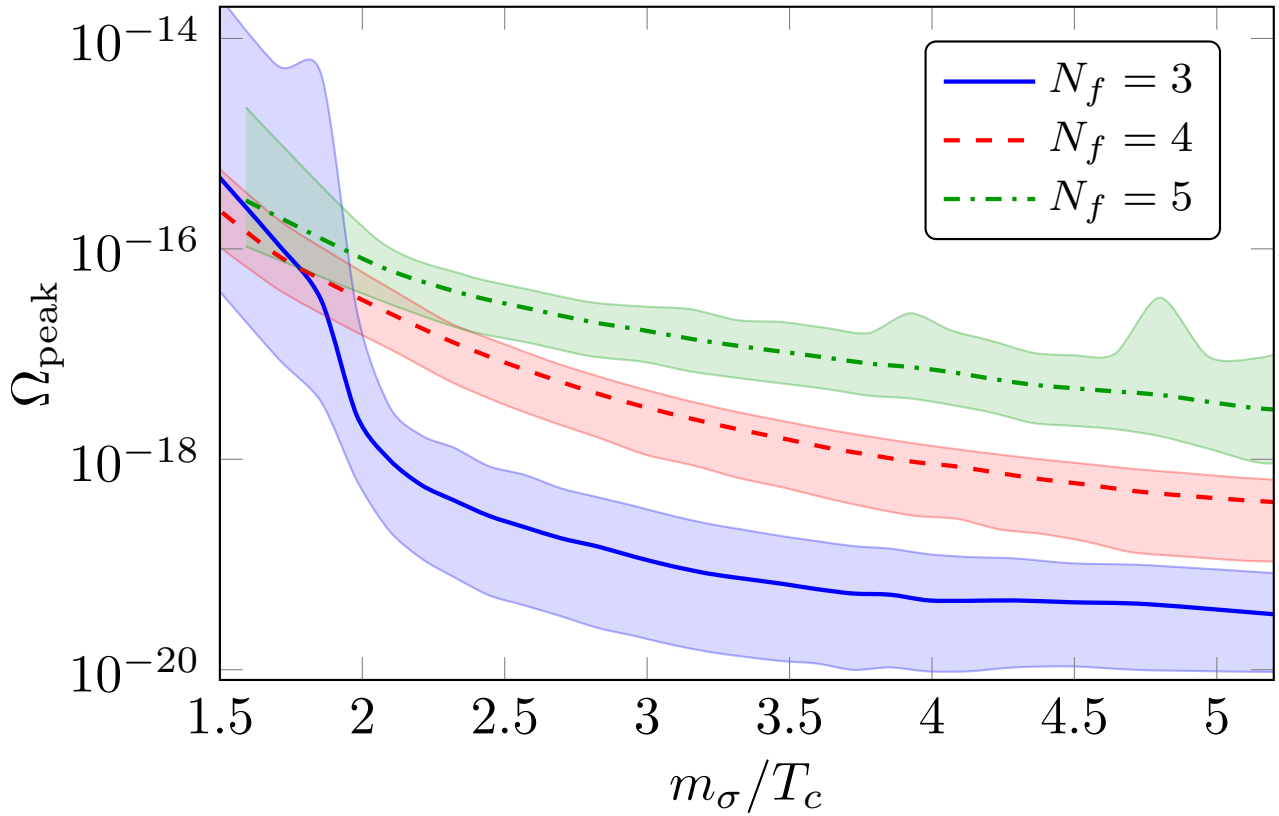

图: We show the averaged values of the peak amplitude $\Omega_{\rm peak}$ as a function of physical observables m_σ in units of T_c in the LSM for $N_f = 3, 4, 5$. The sigma meson mass has the strong correlation with the peak amplitude: smaller values of m_σ lead to a larger $\Omega_{\rm peak}$. The strongest signal can almost reach LISA sensitiviity.

Understanding from Thin Wall Approximation

- The three-dimensional Euclidean action S_3 can be written as a function of the latent heat L and the surface tension σ

$$S_3 = \frac{16\pi}{3}\frac{\sigma(T_c)^3}{L(T_c)^2}\frac{T_c^2}{(T_c - T)^2}\,,$$

- The ratio $S_3(T_p)/T_p$ is typically a number $\mathcal{O}(150)$ for phase transitions around the electroweak scale and the inverse duration $\tilde{\beta}$ follows as

$$\tilde{\beta} = T\frac{\mathrm{d}}{\mathrm{d}T}\frac{S_3(T)}{T}\bigg|_{T=T_p} \approx \mathcal{O}(10^3)\frac{T_c^{1/2}L}{\sigma^{3/2}}\,.$$

- $\tilde{\beta}$ stems from the competition between the surface tension and latent heat. $L \sim N^2$ while σ can be either $\sigma \sim N$ or $\sigma \sim N^2$ with limited data up to $SU(8)$
- How to construct models with smaller latent heat and larger surface tension to enhance the gravitational wave signals?

Third Part: Glueball Dark Matter Production Mechanism

Motivation: Why Glueball Dark Matter?

- A pure dark Yang–Mills sector is arguably the **simplest confining dark sector**.
- Once the theory confines, it inevitably produces a tower of **glueball bound states**.
- In the absence of dark fermions, the glueballs are **cleanly defined**: there are no mesons, baryons, or fermionic bound states that can mix with them.
- This makes the low-energy spectrum theoretically **simple**, **predictive**, and directly tied to the confinement scale.
- Lattice studies indicate that the scalar 0^{++} glueball is the **lightest state** in the spectrum.
- Therefore, in a sufficiently secluded dark sector, the lightest 0^{++} glueball naturally becomes the leading **dark-matter candidate**.

Minimal logic

$$\text{pure } SU(N)_D \text{ Yang-Mills}$$

$$\Downarrow \text{ confinement}$$

$$\text{glueball tower}$$

$$0^{++} \text{ lightest}$$

$$\Longrightarrow \text{ DM candidate}$$

Take-home message

Glueball dark matter is minimal, clean, and predictive: confinement alone is enough to generate a well-defined dark-matter candidate.

Rigorous Dark Gluon-glueball Dynamics

(Carenza, Pasechnik, Salinas，Z-W W, Phys. Rev. Lett. **129** (2022) no.26, 26)

- In the literature, for glueball dark matter production, only ϕ^5 interaction is considered, making the $3 \to 2$ annihilation the only relevant process for DM formation
- However, since glueball is strongly coupled, this naive calculation is not rigorous. A non-perturbative method is required.
- The dark gluon-glueball dynamics can be effectively described by considering the dimension-4 glueball field $\mathcal{H} \propto \text{tr}(G^{\mu\nu}G_{\mu\nu})$:

$$V\left[\mathcal{H},\ell\right] = \frac{\mathcal{H}}{2}\ln\left[\frac{\mathcal{H}}{\Lambda^4}\right] + T^4\mathcal{V}\left[\ell\right] + \mathcal{H}\mathcal{P}[\ell] + V_T\left[\mathcal{H}\right] .$$

- We keep the lowest order in $\mathcal{P}[\ell]$ to satisfy the symmetry:

$$\mathcal{P}[\ell] = c_1|\ell|^2 ,$$

where c_1 is determined by the lattice results (jumping of gluon condensate).

Thermal evolution of the dark gluon-glueball system

(Carenza, Pasechnik, Salinas， Z-W W, Phys. Rev. Lett. **129** (2022) no.26, 26)

- Introducing canonically normalized glueball field, we introduce ϕ as $\mathcal{H} = 2^{-8}c^{-2}\phi^4$ and the effective Lagrangian reads:

$$\mathcal{L} = \frac{c}{2}\frac{\partial_\mu \mathcal{H}\partial^\mu \mathcal{H}}{\mathcal{H}^{3/2}} - V[\mathcal{H},\ell] \Rightarrow \frac{1}{2}\partial_\mu\phi\partial^\mu\phi - V[\phi,\ell]\,,$$

$$V[\phi,\ell] = \frac{\phi^4}{2^8c^2}\left[2\ln\left(\frac{\phi}{\Lambda}\right) - 4\ln 2 - \ln c\right] + \frac{\phi^4}{2^8c^2}\mathcal{P}[\ell] + T^4\mathcal{V}[\ell] \quad ,\mathcal{P}[\ell] = c_1|\ell|^2$$

$$\mathcal{V}[\ell] = T^4\left(-\frac{b_2(T)}{2}|\ell|^2 + b_4|\ell|^4 + \cdots - b_3\left(\ell^N + \ell^{*N}\right)\right),$$

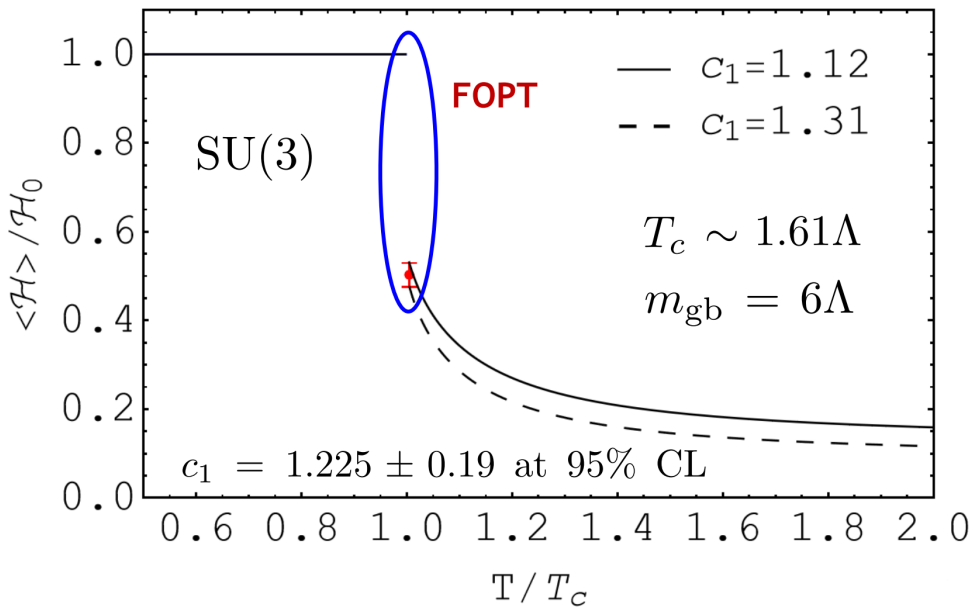

Cosmological evolution of the dark glueball field

(Carenza, Pasechnik, Salinas， Z-W W, Phys. Rev. Lett. **129** (2022) no.26, 26)

- The glueball field is considered homogeneous and evolves in expanding FLRW universe, with the E.O.M.

$$\ddot{\phi} + 3H\dot{\phi} + \partial_\phi V[\phi, T] = 0\,,$$

- The time variable is found in terms of the photon temperature:

$$t = \frac{1}{2}\sqrt{\frac{45}{4\pi^3 g_{*,\rho}(T_\gamma)}}\frac{m_P}{T_\gamma^2}\,, \qquad T_\gamma = \xi_T T$$

where ξ_T denotes the visible-to-dark sector temperature ratio and $m_P = 1.22 \times 10^{19}$ GeV is the Planck mass and $g_{*,\rho}$ is the number of energy-related degrees of freedom.

- E.O.M. in terms of the dark sector temperature:

$$\frac{4\pi^3 g_{*,\rho}}{45 m_P^2}\xi_T^4 T^6 \frac{d^2\phi}{dT^2} + \frac{2\pi^3}{45 m_P^2}\frac{dg_{*,\rho}}{dT}\xi_T^4 T^6 \frac{d\phi}{dT} + \partial_\phi V[\phi, T] = 0$$

Cosmological Evolution of the Dark Glueball Field

(Carenza, Pasechnik, Salinas， Z-W W, Phys. Rev. Lett. **129** (2022) no.26, 26)

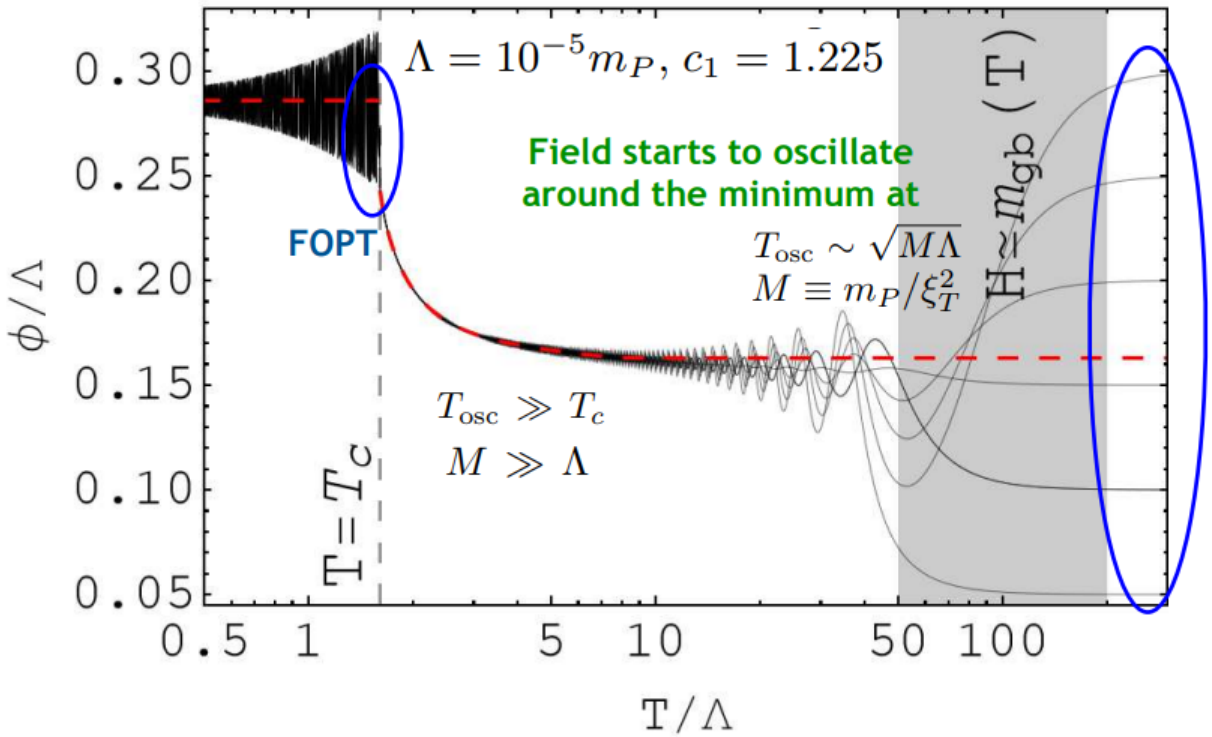

- Field starts to oscillate around the minimum of the potential when $H \simeq m_{\rm gb}$ with temperature $T_{\rm OSC} \sim \sqrt{M\Lambda}$
- In early times in deconfined regime, for different initial conditions the field evolution follows the minimum (red dashed line).
- First order phase transition washes out any dependence on initial conditions.

Glueball Relic Density

(Carenza, Pasechnik, Salinas， Z-W W, Phys. Rev. Lett. **129** (2022) no.26, 26)

- Energy stored in these oscillations around $\phi_{\rm min} \approx 0.28\Lambda$ is the relic DM abundance, $\Omega h^2 = \rho/\rho_c$ (critical density $\rho_c = 1.05 \times 10^4\,{\rm eV\,cm^{-3}}$)

$$\rho = \frac{2\pi^3}{45} g_{*,\rho}(T) \frac{T^6}{M^2} \left(\frac{d\phi}{dT}\right)^2 + V[\phi]\,.$$

- Then the relic density today is calculated (f denotes as final):

$$\Omega h^2 = \frac{\Lambda}{\rho_c/h^2} \left\langle \frac{\tilde{\rho}}{\tilde{T}^3} \right\rangle_f T_f^3 \left(\frac{T_{\gamma,0}}{\zeta_T T_f}\right)^3 = 0.12 \zeta_T^{-3} \frac{\Lambda}{\Lambda_0}\,,$$

  with dilution factor $(T_{\gamma,0}/\zeta_T T_f)^3$ to consider the Universe expansion
- Below freeze-out temperature, the predicted glueball relic density is

$$0.12\zeta_T^{-3} \frac{\Lambda}{137.9\,{\rm eV}} \lesssim \Omega h^2 \lesssim 0.12\zeta_T^{-3} \frac{\Lambda}{82.7\,{\rm eV}}, \quad 1.035 < c_1 < 1.415$$

  for $\zeta_T^{-1} = 0.1$, the glueball dark matter mass $M_{\rm gl} \sim 6\Lambda$ is $\sim 0.1{\rm MeV}$
- It is more than a factor of 10 difference compared to the old calculations

$$\Omega h^2 \sim 0.12\,\zeta_T^{-3} \frac{\Lambda}{5.45\,{\rm eV}}$$

Glueball Dark Matter Parameter Space (no portal)

(Carenza, Pasechnik, Salinas，Z-W W, Phys. Rev. Lett. **129** (2022) no.26, 26;

(Carenza, Ferreira, Pasechnik and Z-W W, Phys. Rev. D **108** (2023) no.12, 12)

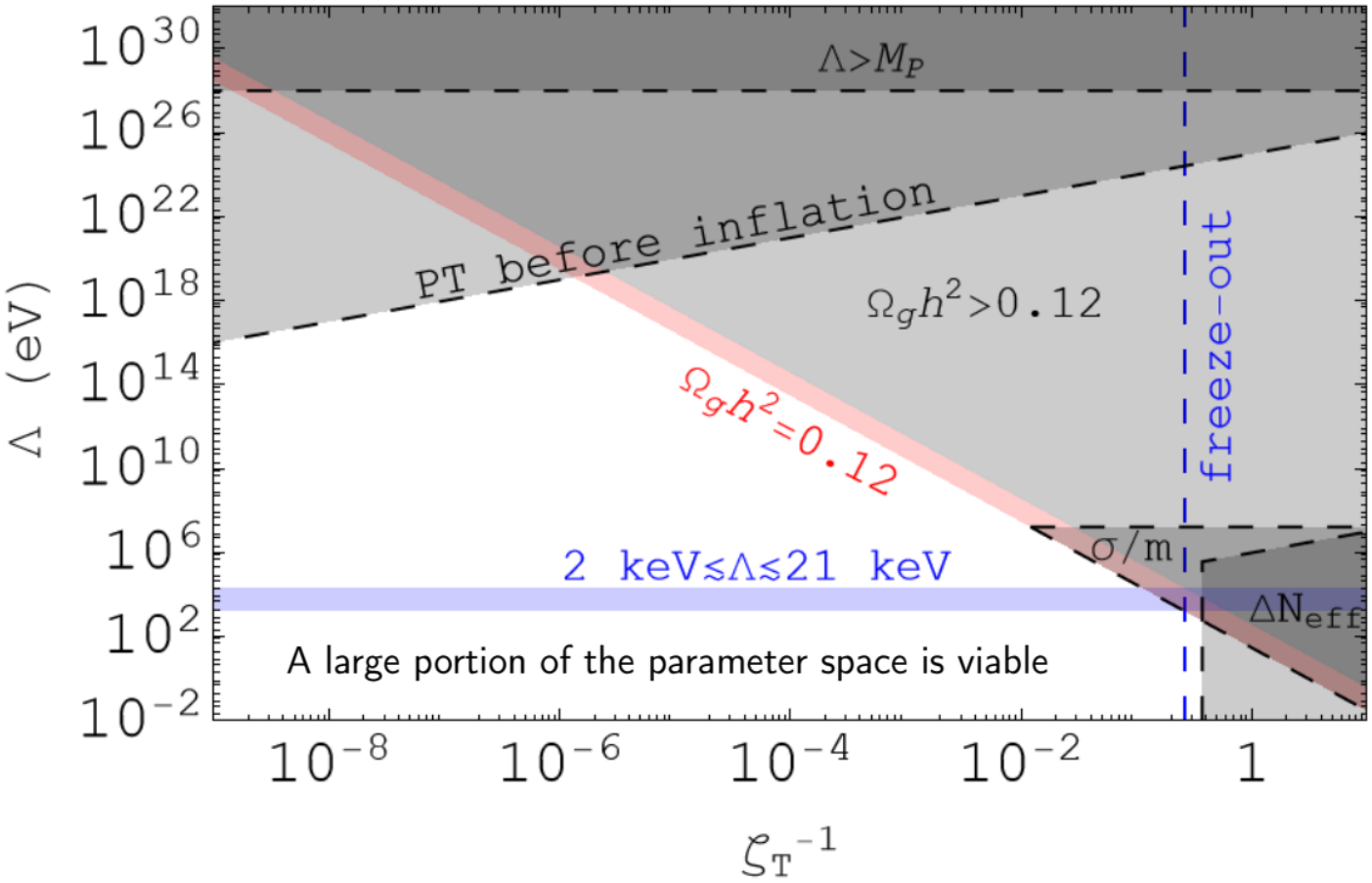

图: The red diagonal band corresponds to the full-DM condition, $\Omega_g h^2 \simeq 0.12$. Points below the band are underabundant: glueballs remain viable, but only as a subdominant DM component.

Fourth Part: Glueball Axion Like Particles (GALPs)

What is a GALP?

GALPs are composite pseudoscalar glueball states—or a mixed glueball mass eigenstate—with ALP-like photon couplings and misalignment-like relic production, but—unlike ordinary axions—their first-order confinement transition washes out the sensitivity to the initial field value. It is composite, naturally heavy, and does not solve the strong-CP problem.

Glueball Spectrum

(Y. Chen *et al.* “Glueball spectrum and matrix elements on anisotropic lattices,” Phys. Rev. D **73** (2006) 014516)

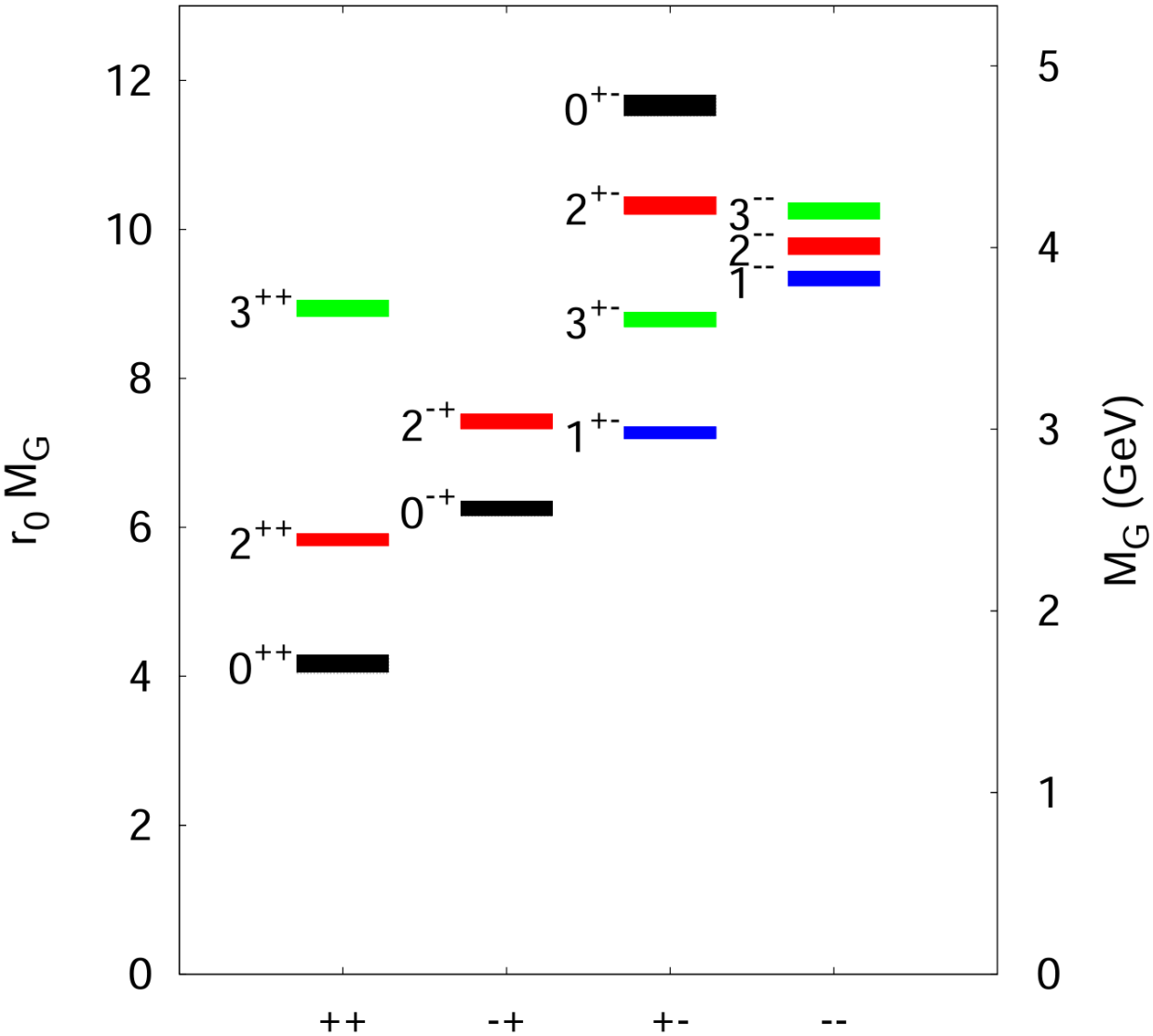

Adding the θ term

(Carenza, Pasechnik, Z-W W, Phys. Rev. Lett. **135** (2025) 021001)

- We can add the θ term to incorporate also the pseudoscalar glueball state $\mathcal{A} \equiv 0^{-+}$

$$\mathcal{L}_{\mathrm{SU(N)}} = -\frac{1}{4} G^a_{\mu\nu} G^{\mu\nu a} + \frac{\theta}{4} G^a_{\mu\nu} \tilde{G}^{\mu\nu a} \,,$$
$$G^a_{\mu\nu} = \partial_\mu A^a_\nu - \partial_\nu A^a_\mu + g f^{abc} A^b_\mu A^c_\nu \,.$$

- We obtain the glueball EFT Lagrangian as (here $\mathcal{H}$ is ϕ before):

$$\mathcal{L}_{\mathrm{eff}} = \frac{1}{2} \partial_\mu \mathcal{H} \partial^\mu \mathcal{H} + \frac{1}{2} \partial_\mu \mathcal{A} \partial^\mu \mathcal{A} - V_{\mathrm{eff}}(\mathcal{H}, \mathcal{A}) \,,$$

  where $\mathcal{H} \equiv 0^{++}$ is the standard scalar glueball state while $\mathcal{A} \equiv 0^{-+}$ denotes the pseudoscalar glueball state.
- Specifically, the 0^{++} and 0^{-+} glueball fields are defined in terms of gauge-invariant operators of the lowest dimension as

$$\mathcal{H}^4 \equiv -\frac{\beta(g)}{2g} G^a_{\mu\nu} G^{\mu\nu a} \,, \quad \mathcal{A}\,\mathcal{H}^3 \equiv G^a_{\mu\nu} \tilde{G}^{\mu\nu a}$$

  in terms of β-function $\beta(g)$.

Why $V_{\rm eff}(H, A)$ Matters for GALP Phenomenology

(Carenza, Pasechnik, Z-W W, Phys. Rev. Lett. **135** (2025) 021001)

- The two-glueball effective potential is not arbitrary: its structure is constrained by the **trace anomaly** together with the nonzero θ term.
- $V_{\rm eff}(H, A)$ fixes the vacuum configuration (η_0, a_0), the mass matrix, and the scalar–pseudoscalar mixing after confinement.
- It also controls low-energy self-interactions and whether the heavier glueball efficiently converts or decays into the lighter one.
- Hence $V_{\rm eff}$ directly affects how we interpret the relic sector: if the heavier state is depleted, DM is effectively single-component; if both states survive, one should think in terms of two-component GALP DM.
- In this sense, $V_{\rm eff}(H, A)$ plays for GALPs the same role that $V[H, \ell]$ played earlier for scalar glueball production: it is the IR engine behind the phenomenology.

Trace-anomaly input

$$\partial_\mu D^\mu = -\Theta^\mu{}_\mu \propto -H^4$$

Potential structure

$$V_{\rm eff} \simeq c_0 \mathcal{H}^4 \ln\left(\frac{\mathcal{H}}{\Lambda}\right) + \frac{\theta}{4}\mathcal{A}\,\mathcal{H}^3 + \mathcal{H}^4 f\left(\frac{\mathcal{A}}{\mathcal{H}}\right) + c_1\mathcal{H}^4 + c_2\mathcal{H}^2\mathcal{A}^2 + c_3\mathcal{A}^4 + c_4\mathcal{H}\,\mathcal{A}^3\,,$$

What it fixes

- vacuum (η_0, a_0)
- mass matrix and mixing
- conversion / decay channels

$\Longrightarrow$ one-component
or
two-component GALP DM

GALP relic abundance: one-component vs two-component DM (Carenza, Pasechnik, Z-W W, Phys. Rev. Lett. **135** (2025) 021001)

- The GALP relic interpretation is not unique: it depends on whether the heavier glueball is depleted before late times.
- **One-component benchmark:** if in-medium decay / conversion is efficient, the heavier state is transferred into the lighter one, and the late-time relic density is effectively that of the lightest glueball.
- **Two-component benchmark:** if both η and a remain cosmologically stable, the scalar-glueball relic estimate can be approximately extended to a two-component DM system.
- In the extended EFT analysis, a realistic simplified benchmark is to assume comparable present-day contributions from η and a. This is especially plausible when θ is non-negligible, so that the pseudoscalar sector is dynamically relevant.

Physical question
What survives after confinement and thermal evolution?

Case A: one-component DM

$$a_{\mathrm{heavy}} \;\to\; \eta_{\mathrm{light}}$$

Late-time DM is dominated by the lightest glueball state.

Case B: two-component DM

$$\eta \;+\; a$$

Both species survive and contribute to the present relic density.

$$\Omega_{\mathrm{DM}} = \Omega_\eta + \Omega_a$$

large mixing+both states survive+no efficient depletion→comparable abundances $\Omega_\eta \sim \Omega_a$

Take-home:
before discussing later phenomenology, the relic-sector composition must be specified.

Why the Heavy Portal Does Not Modify IR Glueball Production

- The portal fermions Ψ are **UV mediators**, not light IR flavors.
- Around $T \sim M_\Psi$, $\Psi\bar{\Psi}$ annihilation / decoupling fixes the dark-visible temperature ratio

$$\zeta_T^{-1} \equiv \frac{T_{\rm dark}}{T_\gamma}, \qquad \Omega_g h^2 \propto \zeta_T^{-3} \Lambda_D.$$

- Their finite-temperature contribution to confinement dynamics is Boltzmann suppressed:

$$\delta V_f \propto e^{-m_\Psi/T} \,\mathrm{Tr}\, L.$$

  Hence the Polyakov-loop potential is close to the **pure Yang–Mills** limit.
- In a sample case,

$$m_\Psi \gtrsim 5T_c \to e^{-m_\Psi/T} \sim 7 \times 10^{-3}$$

  so the late-time IR remains **effectively pure Yang–Mills**.
- Cosmologically, the symmetric $\Psi\bar{\Psi}$ abundance is efficiently depleted; any tiny residual around T_c is further reduced by confinement / bound-state effects.

Portal: two jobs

$$\frac{\tau\alpha^2}{M_\Psi^4} G_D^2 F^2 \quad \Longrightarrow \quad \text{EFT portal}$$

$$\Psi\bar{\Psi}\ \text{annihilation} \quad \Longrightarrow \quad \zeta_T$$

What changes vs. what doesn't

Modified: thermal history, ζ_T, EFT matching

Unmodified: IR glueball formation mechanism

Main consequence

The portal fermions modify ζ_T, not the IR glueball-production dynamics.

Therefore the previous PRL glueball-production framework can still be used.

The Portal's Two Jobs: Coupling and Thermal History

- To connect the dark Yang–Mills sector to the SM, introduce a heavy Dirac fermion Ψ carrying both dark color and electric charge.
- Integrating out Ψ above the confinement scale generates dim-8 gauge portals between the dark gluon operators and photons.
- After confinement, the same portal induces the effective GALP–photon coupling discussed on the next slide.
- But the portal does more than coupling: it also controls the thermal contact between the visible and dark sectors.
- Around $T \sim M_\Psi$, annihilation / decoupling of $\Psi\bar{\Psi}$ fixes the dark-visible temperature ratio

$$\zeta_T^{-1} \equiv \frac{T_{\rm dark}}{T_\gamma}.$$

- Hence the portal feeds both the EFT coupling *and* the abundance condition used later to obtain the full-DM mass–coupling relation.

Job 1: low-energy coupling

$$\mathcal{L}_{\rm eff} \supset \frac{\tau^2 \alpha^2}{M_\Psi^4}\left(c_\gamma\, G^2 F^2 + \tilde{c}_\gamma\, G\tilde{G}\, F\tilde{F}\right)$$

$$\Longrightarrow \qquad g_{a\gamma} \sim \kappa\, \alpha^2\, \Lambda^{-1} \left(\frac{\Lambda}{M_\Psi}\right)^4$$

Job 2: thermal history

$\Psi\bar{\Psi}$ annihilation/decoupling $\Longrightarrow$ ζ_T

$$\Omega_{\rm GALP} h^2 \propto \zeta_T^{-3}\, \Lambda \qquad \text{(schematically)}$$

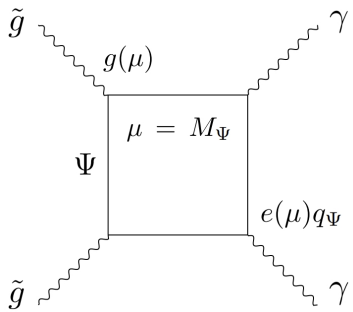

The portal sets both the coupling and the cosmological benchmark.

Effective PQ-like Scale

(Carenza, Pasechnik, Z-W W, Phys. Rev. Lett. **135** (2025) 021001)

- $$\mathcal{L}_{\rm eff} \supset \frac{\tau^2\alpha^2}{M_\Psi^4}\left[c_\gamma\, G^a_{\mu\nu}G^{\mu\nu a}F_{\alpha\beta}F^{\alpha\beta} + \tilde{c}_\gamma\, G^a_{\mu\nu}\tilde{G}^{\mu\nu a}F_{\alpha\beta}\tilde{F}^{\alpha\beta}\right].$$
- Linearizing around the VEVs (η_0, a_0) and keeping only terms linear in a, η:

$$G^a_{\mu\nu}G^{\mu\nu a} = -\frac{8g\eta_0^3\,\eta}{\beta(g)}\,, \quad G^a_{\mu\nu}\tilde{G}^{\mu\nu a} = \eta_0^3 a + 3a_0\eta_0^2\eta\,.$$

- Turning to the mass basis $\{\eta, a\} \to \{\phi_1, \phi_2\}$, we obtain:

$$\mathcal{L}_{\rm eff} \supset \frac{1}{4}\sum_{i=1,2}\left[g_{\phi_i\gamma}\,\phi_i F_{\mu\nu}F^{\mu\nu} + \tilde{g}_{\phi_i\gamma}\,\phi_i F_{\mu\nu}\tilde{F}^{\mu\nu}\right].$$

- The effective couplings satisfy $g_{\phi_i\gamma} \sim \tilde{g}_{\phi_i\gamma} \equiv g_{\rm GALP\gamma}$, where

$$g_{\rm GALP\gamma} = \kappa\,\alpha^2\Lambda^{-1}\left[\frac{\Lambda}{M_\Psi}\right]^4 = 2.45\times10^{-7}\,{\rm GeV}^{-1}\,\kappa\left[\frac{m_{\rm GALP}}{\rm GeV}\right]^3\left[\frac{M_\Psi}{\rm GeV}\right]^{-4}.$$

- The PQ-like scale is thus obtained ($f_a \propto g^{-1}_{\rm GALP\gamma}$):

$$f_a \simeq 4.1\times10^3\ {\rm GeV}\,\kappa^{-1}\left[\frac{\Lambda}{\rm GeV}\right]^{-3}\left[\frac{M_\Psi}{\rm GeV}\right]^4.$$

GALP DM Mass–Coupling Relation

(Carenza, Pasechnik, Z-W W, “Composite Heavy Axionlike Dark Matter" PRL 135 (2025) 021001)

Analytic relation

$$g_{\mathrm{GALP}\gamma} \simeq 2.5 \times 10^{-7}\,\mathrm{GeV}^{-1}\,\kappa\left(\frac{m_{\mathrm{GALP}}}{\mathrm{GeV}}\right)^{3}\left(\frac{M_\Psi}{\mathrm{GeV}}\right)^{-4}$$

$$f_a^{\mathrm{eff}} \simeq 4.1 \times 10^{3}\,\mathrm{GeV}\,\kappa^{-1}\left(\frac{\Lambda}{\mathrm{GeV}}\right)^{-3}\left(\frac{M_\Psi}{\mathrm{GeV}}\right)^{4}$$

- This is the defining relation of the GALP setup.
- For fixed M_Ψ, heavier GALPs imply a larger photon coupling.
- For fixed m_{GALP}, increasing M_Ψ strongly suppresses $g_{\mathrm{GALP}\gamma}$.
- The full-DM region is selected by cosmological stability and self-interaction bounds.
- GALPs therefore occupy a heavy-mass / tiny-coupling window beyond the standard ALP paradigm.

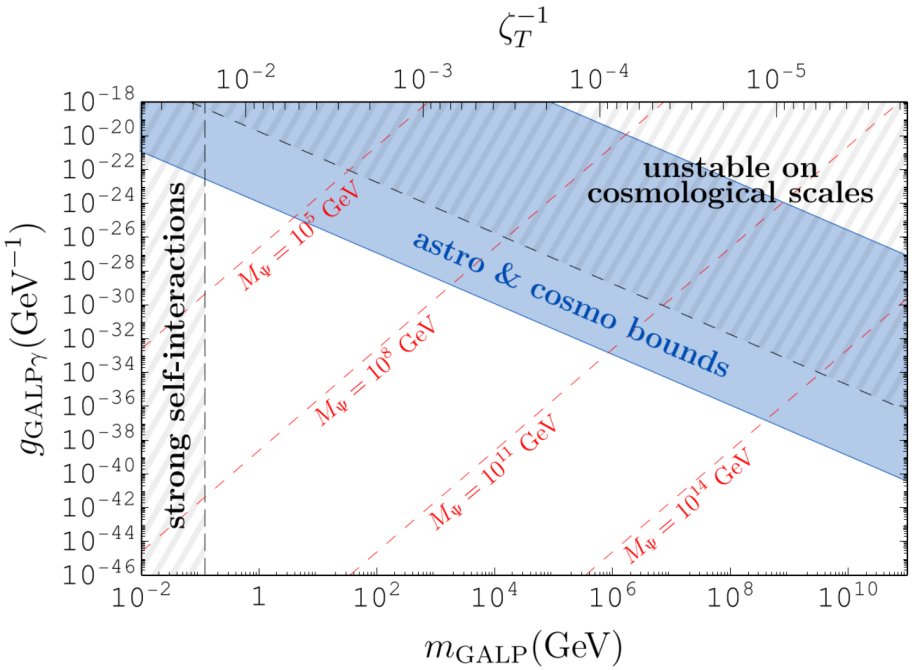

Take-home:
GALPs naturally realize heavy composite ALP DM with an emergent, effectively super-Planckian PQ-like scale.

Fifth Part: Glueball Direct Detection

Why Direct Detection Favors C-odd Oddballs

(Li, Pasechnik, Wang and Z-W W, arXiv:2602.18753 (submitted to PRL)

Two benchmark portal scenarios

Scenario I: a single charged fermion portal with a heavy mediator

$\Longrightarrow$ *radiative decays persist*

and direct detection is strongly suppressed.

Scenario II: a two-flavor vector-like portal with approximate global $SU(2)_D$ and opposite electric charges

$\Longrightarrow$ *oddball DM can be stable*

while elastic scattering still survives.

Why oddballs can be stable yet detectable

- The relevant DM candidates are the lightest C-odd oddballs, e.g. 1^{+-} and 1^{--}.
- **Step 1:** their leading *linear* portal operators involve an **odd number of photons**, not an F^2-type two-photon structure; hence the usual box-induced $\chi \to \gamma\gamma$ channel is not the relevant leading decay route.
- **Step 2:** in the approximate $SU(2)_D$ limit, $Q_{\psi_+} = -Q_{\psi_-}$ implies $Q_{\psi_+}^{2n+1} + Q_{\psi_-}^{2n+1} = 0$, so all **single-oddball odd-photon** amplitudes cancel.
- Therefore radiative cascades such as $1^{+-}, 1^{--} \to 0^{++} + \gamma$ are forbidden, while the bilinear $\chi\chi\gamma\gamma$ amplitude relevant for elastic scattering still survives.

J^{PC}	Mass/$m_{0^{++}}$	Decay operator	Scaling	Portal
$\mathbf{0^{++}}$	1	G^2F^2	$\alpha_D^2\alpha^2\,\Lambda_D^9 m_\psi^{-8}$	I
$\mathbf{0^{-+}}$	~ 1.55	$G\tilde{G}F\tilde{F}$		
$\mathbf{0^{+-}}$	~ 2.7	G^3F	$\alpha_D^3\alpha\,\Lambda_D^9 m_\psi^{-8}$	I/II
		G^3F^3	$\alpha_D^3\alpha^3\,\Lambda_D^{17} m_\psi^{-16}$	
$\mathbf{0^{--}}$	—	$\tilde{G}G^2F$	$\alpha_D^3\alpha\,\Lambda_D^9 m_\psi^{-8}$	
		$\tilde{G}G^2\tilde{F}F^2$	$\alpha_D^3\alpha^3\,\Lambda_D^{17} m_\psi^{-16}$	
$\mathbf{1^{++}}$	—	G^3F	$\alpha_D^3\alpha\,\Lambda_D^9 m_\psi^{-8}$	I/II^a
$\mathbf{1^{-+}}$	~ 2.49			
$\mathbf{1^{+-}}$	~ 1.78	G^3F	$\alpha_D^3\alpha\,\Lambda_D^9 m_\psi^{-8}$	I/II
		G^3F^3	$\alpha_D^3\alpha^3\,\Lambda_D^{17} m_\psi^{-16}$	
$\mathbf{1^{--}}$	~ 2.44	$\tilde{G}G^2F$	$\alpha_D^3\alpha\,\Lambda_D^9 m_\psi^{-8}$	
		$\tilde{G}G^2\tilde{F}F^2$	$\alpha_D^3\alpha^3\,\Lambda_D^{17} m_\psi^{-16}$	

Table I of arXiv:2602.18753. C-even states use two-photon operators, while C-odd oddballs use odd-photon operators.

Pomeron Foundation I: Why the Problem is Non-Perturbative

(Li, Pasechnik, Wang and Z-W W, arXiv:2602.18753 (submitted to PRL)

Coulomb-regime elastic scattering and amplitude

In the Galactic DM regime, the coherent process

$$\chi A \to \chi A$$

is dominated by **two off-shell photons**.
The corresponding elastic amplitude is

$$\mathcal{M}_\chi \propto \int \frac{d^4k}{(2\pi)^4} \frac{J_A^\mu(k_1)\, J_A^\nu(k_2)\, T^\chi_{\mu\nu}(p,q;k)}{(k_1^2+i\epsilon)(k_2^2+i\epsilon)}.$$

- J_A^μ: elastic nuclear current, with $J_A^\mu(k) = (P+P')^\mu F_A(Q^2)$
- $T^\chi_{\mu\nu}$: doubly-virtual glueball Compton tensor

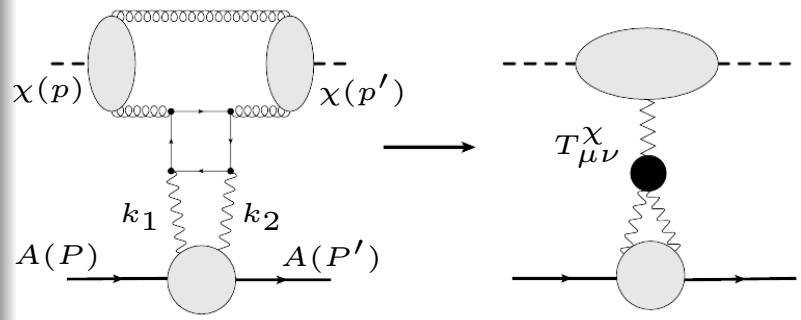

Fig. 2 of arXiv:2602.18753

Why non-perturbative input is necessary

- The **nuclear side** is under control through coherent Coulomb scattering and elastic form factors.
- The **glueball side** is difficult: it contains the long-distance response of a confining dark Yang–Mills state.
- The dim-8 portal matching determines the short-distance piece, but the full scattering amplitude still needs a controlled treatment of **non-perturbative glueball physics**.
- This is exactly why the paper introduces a QCD-inspired dark tensor-Pomeron framework in the next step.

Pomeron Foundation II: Dark Tensor Pomeron as the EFT Bridge

(Li, Pasechnik, Wang and Z-W W, arXiv:2602.18753 (submitted to PRL)

- For $m_\psi \gtrsim \frac{1}{2}m_{1^{+-}} \sim 5.5\Lambda_D$, the infrared dynamics is effectively pure Yang–Mills, so the forward vacuum exchange is expected to be **dominated by a gluonic dark Pomeron**.
- In the forward regime, the doubly-virtual glueball Compton tensor is modeled by a **soft spin-2 dark Pomeron** in the Ewerz–Maniatis–Nachtmann (EMN) framework.
- This gives a controlled bridge between **UV portal matching** and the **non-perturbative glueball response** relevant for direct detection.
- Crucially, the long-distance part is not put in by hand. Instead, it is based on QCD soft-scattering phenomenology and then systematically **rescaled** to the dark sector.
- So the direct-detection amplitude is calculable in a way that keeps both **factorization** and **gauge invariance** manifest.

Short $\times$ long factorization

$$T^{\chi}_{\mu\nu} \sim \left[\gamma^*\gamma^* \to g_D g_D\right]_{\text{short}} \times \langle\chi|G^2_D|\chi\rangle_{\text{long}}$$

$$\Downarrow \quad \text{forward regime}$$

$$T^{\mu\nu}_{\chi} \sim \Gamma^{(\gamma\gamma P_D)}_{\mu\nu\kappa\lambda}\, \Delta^{(P_D)\kappa\lambda,\rho\sigma}\, \Gamma^{(\chi\chi P_D)}_{\rho\sigma}\, F_{\text{el}}(t)$$

$$k_{1\mu}\Gamma^{\mu\nu\kappa\lambda} = 0, \qquad k_{2\nu}\Gamma^{\mu\nu\kappa\lambda} = 0$$

Dark-sector Rescaling

- Pomeron intercept ϵ_D
- Regge slope α'_D
- $\gamma\gamma P_D$ couplings
- $\chi\chi P_D$ couplings
- elastic slope b^D_{eff}

Predicted Xenon Reach

(Li, Pasechnik, Wang and Z-W W, arXiv:2602.18753 (submitted to PRL)

- After the non-perturbative matching, the spin-independent per-nucleon cross section scales as $\sigma_{\rm SI} \propto \Lambda_D^{2.15}\, m_\psi^{-8}$.
- Current and next-generation Xenon sensitivity $\sigma_{\rm SI} \sim 10^{-46}$–$10^{-48}\ {\rm cm}^2$ roughly corresponds to

  $m_\psi \sim 3$–$30\ {\rm GeV}$,

  $\Lambda_D \sim 0.55$–$5.5\ {\rm GeV}$.
- Present PandaX already probes approximately $m_\psi \lesssim 20\ {\rm GeV}$, while PandaX-xT can extend the reach to $m_\psi \sim 30\ {\rm GeV}$.
- Glueball stability simultaneously requires $m_\psi > 5.5\,\Lambda_D$.

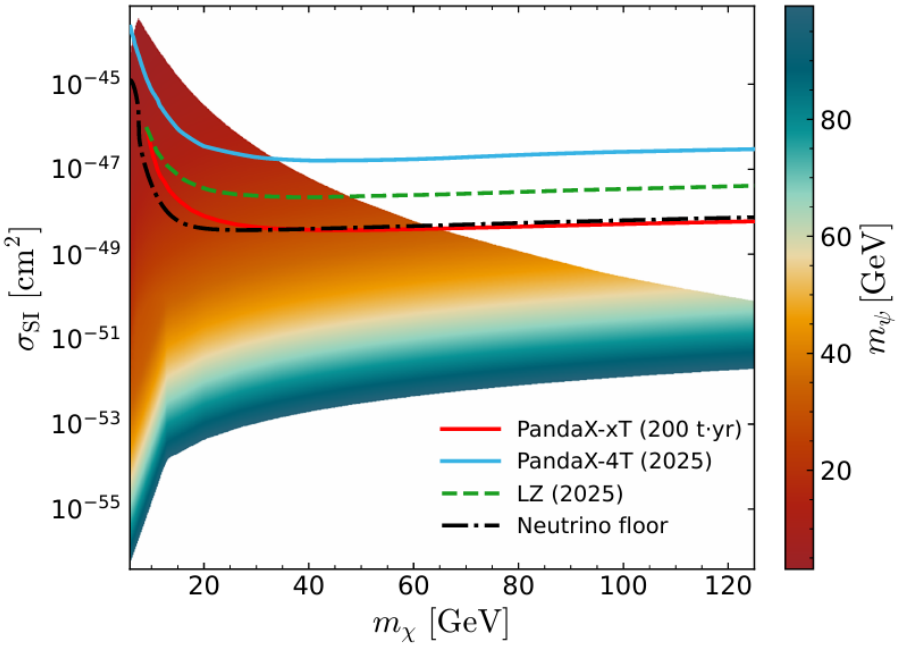

Fig. 3: Direct-detection reach for dark glueball DM.

Why a Light Charged Portal Is Not Immediately Ruled Out

Key physical picture

- LEP2 production is dominantly neutral-current:

$$e^+e^- \to \gamma^*/Z^* \to U\bar{U},\ D\bar{D},$$

  so the primary state is overall electrically neutral.
- Since the produced fermions also carry dark color, the pair is immediately connected by a dark string and forms a compact quirkonium-like bound state, rather than two macroscopic charged tracks.
- The characteristic pullback scale is

$$\sigma \sim \Lambda_{\rm dark}^2, \qquad L_{\rm max} \sim E_{\rm rel}/\sigma, \qquad t_{\rm pull} \sim L_{\rm max}.$$

  For $\Lambda_{\rm dark} \sim 10\,\mathrm{GeV}$, one finds

$$L_{\rm max} \sim (0.02\text{–}0.2)\,\mathrm{fm}, \qquad t_{\rm pull} \lesssim 10^{-24}\,\mathrm{s},$$

  i.e. bound-state formation is immediate on detector scales.

Why charged bound states are hard to make

- Charged open-flavor states such as $U\bar{D}$ require extra pair creation from the dark string, which is Schwinger suppressed: $P_{\rm break} \propto \exp\left[-\pi\, m_\psi^2/\sigma\right]$.
- Charged-current conversion $\bar{U} \to \bar{D} + W^{-*}$ during the strong cooling stage is also too slow: $P_{\rm CC}^{\rm during\ cool} \sim \Gamma_{\rm weak}/\Gamma_{\rm cool} \lesssim 10^{-8}\,\kappa_W^2$

Collider implication

- The dominant bound states produced from neutral-current events remain electromagnetically neutral.
- Therefore the light charged portal is *not* generically excluded as a pair of free heavy stable charged particles.
- What LEP2 mainly probes is the subsequent dark-shower / glueball topology:
  - prompt 0^{++} decay $\to$ visible activity,
  - displaced 0^{++} decay $\to$ LLP-like photons / vertices,
  - escaping 0^{++} $\to$ mono-γ + MET.

Light-Portal UV Completion: Model Sketch

- Goal: keep a light charged portal

$$m_\psi \sim \mathcal{O}(10\text{–}20\ \mathrm{GeV})$$

  without immediate exclusion by LEP/LHC.
- Embed the portal into a split-mixing singlet–doublet completion.
- Add two singlets U, D, two vector-like doublets Ψ_U, Ψ_D, one extra scalar doublet Φ, and a Z_2 symmetry.
- The portal Yukawa is not attached directly to the SM Higgs H, but is sequestered into the extra scalar doublet Φ.
- After EWSB, only two charged mixings are generated:

$$\psi_{U_+} \leftrightarrow U, \qquad \psi_{D_-} \leftrightarrow D.$$

- **Key idea:** the light portal is part of a controlled EW completion, rather than an ad hoc light charged state.

Field content

$$U \sim (\mathbf{1}, +1/2), \qquad D \sim (\mathbf{1}, -1/2),$$
$$\Psi_U \sim (\mathbf{2}, 0), \qquad \Psi_D \sim (\mathbf{2}, 0)$$

$$\Phi = \begin{pmatrix} \phi^+ \\ (v_\Phi + \phi + ia)/\sqrt{2} \end{pmatrix}$$

Z_2 assignment

	H	Φ	Ψ_U	Ψ_D	U	D
Z_2	$+$	$-$	$+$	$-$	$-$	$+$

Portal Yukawas

$$\mathcal{L}_Y \supset -y_U\, \overline{\Psi}_U \widetilde{\Phi}\, U - y_D\, \overline{\Psi}_D \Phi\, D + \mathrm{h.c.}$$

$$\delta_U = \frac{y_U v_\Phi}{\sqrt{2}}, \qquad \delta_D = \frac{y_D v_\Phi}{\sqrt{2}}$$

Why This Completion Survives LEP/LHC

- The two light charged eigenstates are

$$\psi_+ = c_+ U + s_+ \psi_{U_+}, \qquad \psi_- = c_- D + s_- \psi_{D_-}.$$

- **Z-phobic window:** the coupling to the Z is controlled by the doublet fractions

$$f_\pm \equiv s_\pm^2.$$

Hence the portal can stay light without carrying full-strength electroweak couplings.

- **No tree-level $W\psi_+\psi_-$:** the W boson acts within each doublet, while ψ_+ and ψ_- come from different mixing blocks.
- **Suppressed Higgs coupling:** since the portal Yukawa sits in Φ, the SM-like Higgs coupling is reduced by the small CP-even mixing angle θ_s.
- **Oblique parameters:** a positive fermionic ΔT is compensated by a negative scalar contribution for a suitable scalar hierarchy.

Constraint map

Z width:	$\propto f_\pm$
W width:	0 at tree level
h width:	$\propto \sin\theta_s$
T parameter:	$\Delta T_{\rm ferm} + \Delta T_{\rm scal}$

Collider interpretation

$$e^+e^- \to \gamma^*/Z^* \to \psi_\pm \bar{\psi}_\pm$$

The portal pair first hadronizes into a neutral hidden bound state. The visible signal is then controlled by the $0^{++} \to \gamma\gamma$ decay length.

prompt:	standard visible activity
displaced:	LLP-like photons/vertices
mono-γ+MET:	if 0^{++} escapes the detector

For the benchmark, $c\tau_{0^{++}} \simeq 5.8\,\mathrm{cm}$, which lies in the displaced window.

Benchmark: displaced regime
$\Rightarrow$ often the hardest to constrain

The light portal survives by suppressing Z, W, h **couplings and placing the signal in the displaced window.**

Take-Home Messages

- Dark Yang–Mills confinement can generate a first-order phase transition and potentially observable gravitational-wave signals.
- The same confining sector also gives a predictive mechanism for scalar glueball relic formation, linking early-Universe dynamics to dark matter abundance.
- Adding the pseudoscalar state and a heavy portal leads to composite heavy ALPs / GALPs with an emergent effective PQ-like scale.
- A detectable direct-detection window is nontrivial: it requires a symmetry-protected light portal, non-perturbative dark tensor Pomeron input, and a collider-safe EW completion.
- The viable region is narrow but testable: Xenon searches, displaced-photon / LLP collider searches, and astrophysical GALP probes are complementary.

One dark Yang–Mills sector can leave signatures in cosmology, direct detection, astrophysics, and colliders at the same time.

已有成员

杜孟林 教授

研究方向：
强子物理与强相互作用、中高能核物理

王志伟 研究员

研究方向：
粒子物理唯象、超出标准模型的新物理

刘晓 教授

研究方向：
量子场论与弦论

杨智 研究员

研究方向：
强子物理与强相互作用、中高能核物理

王金伟 副教授

研究方向：
暗物质唯象、超出标准模型的新物理

Francesco Sannino
丹麦皇家科学院院士与芬兰科学院院士、电子科技大学名誉教授

研究方向：粒子物理理论与唯象学，超越标准模型的新物理，量子场论

金晟洙 研究员

研究方向：
量子场论与弦论

Thank you for your attention!

New Progresses in Columbia Plot

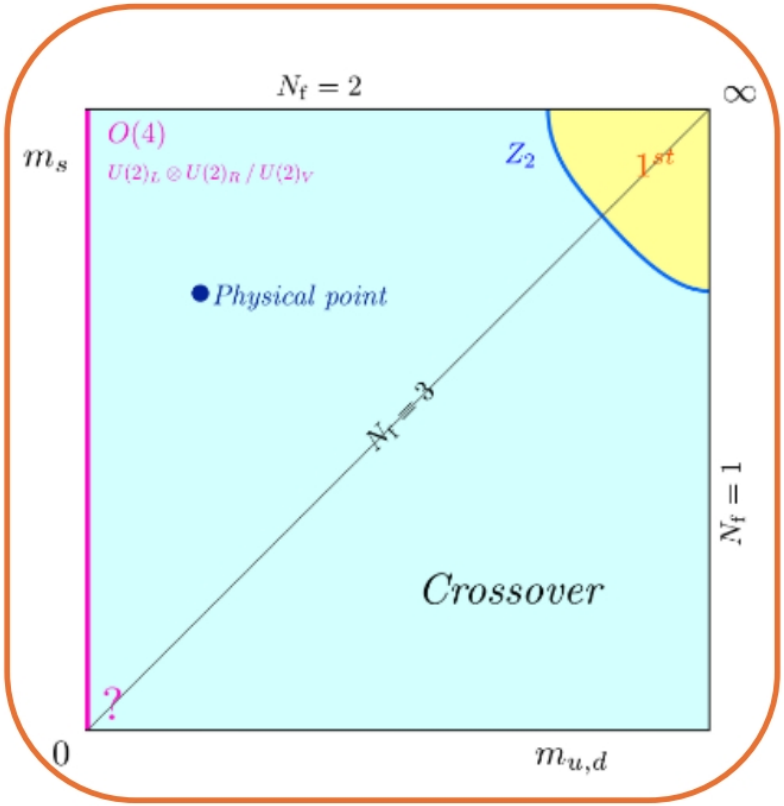

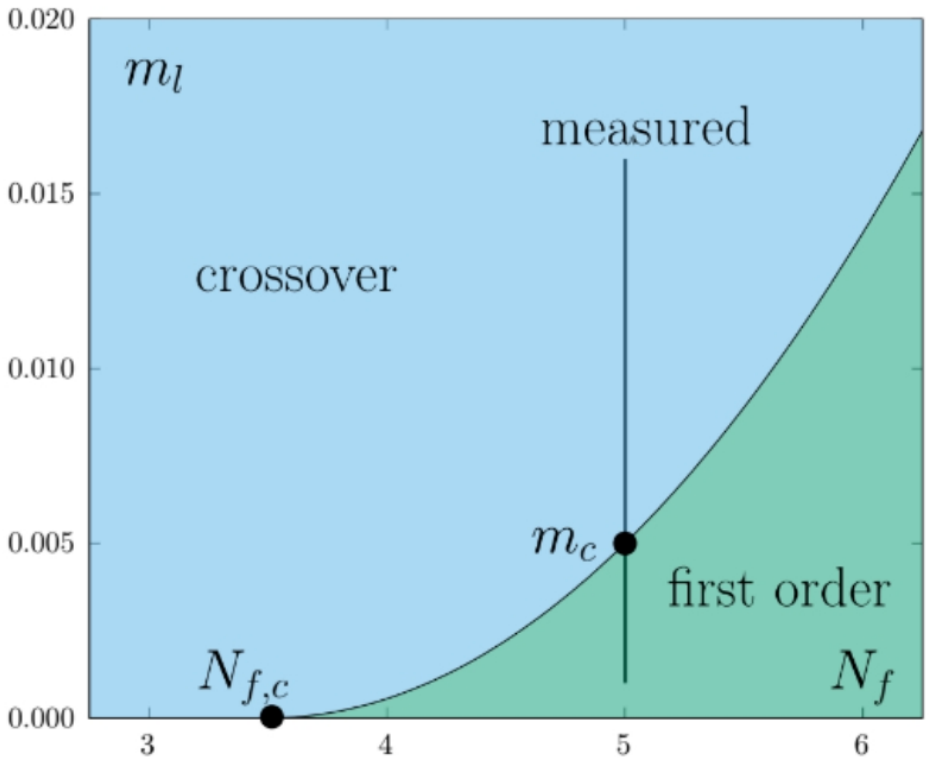

图: Left Fig. Columbia plot from JHEP 11 (2021) 141. Staggered fermions used. Right Fig. from PoS **LATTICE2022** (2023) 027.

About Center Symmetry and Confinement

- The standard physical interpretation is that it is related to the free energy of adding an external static color source in the fundamental representation.

$$\ell\left(\vec{x}\right) = \exp\left(-\mathrm{F}\beta\right)$$

- In the confinement phase, Polyakov loop is zero corresponds to infinity free energy to add a color source and the same time center symmetry is unbroken.

Center Symmetry $Z(N)$ at Nonzero Temperature

- The boundary conditions in imaginary time τ the fields must satisfy are:

$$A_\mu(\vec{x},\beta) = +A_\mu(\vec{x},0), \qquad q(\vec{x},\beta) = -q(\vec{x},0),$$

where gluons as bosons must be periodic in τ while quarks as fermions must be anti-periodic.

- 't Hooft first noticed that one can consider more general gauge transformations which are only periodic up to Ω_c

$$\Omega(\vec{x},\beta) = \Omega_c, \quad \Omega(\vec{x},0) = 1 \qquad \left(\text{here, } \Omega_c = e^{i\phi} I,\ \phi = \frac{2\pi j}{N}\right).$$

- Color adjoint fields are invariant under this transformation, while those in the fundamental representation are not:

$$A^\Omega(\vec{x},\beta) = \Omega_c^\dagger A_\mu(\vec{x},\beta)\,\Omega_c = A_\mu(\vec{x},\beta) = +A_\mu(\vec{x},0),$$
$$q^\Omega(\vec{x},\beta) = \Omega_c^\dagger q(\vec{x},\beta) = e^{-i\phi} q(\vec{x},\beta) \neq -q(\vec{x},0).$$

- Thermal Wilson line transforms like an adjoint field under local $SU(N)$ gauge transformations:

$$L(x) \to \Omega^\dagger(\vec{x},\beta)\, L(\vec{x}) \Omega^\dagger(\vec{x},0).$$

Why is the Polyakov loop the exponential of the static-quark free energy?

Core formulas

First define the temporal Wilson line around the thermal circle:

$$W(\mathbf{x}) = \mathcal{P}\exp\left(ig\int_0^\beta d\tau\, A_0(\tau,\mathbf{x})\right), \qquad \ell(\mathbf{x}) = \frac{1}{N_c}\operatorname{Tr} W(\mathbf{x}).$$

For a static heavy quark, the Euclidean action can be written as

$$S_Q = \int_0^\beta d\tau\, Q^\dagger(\tau,\mathbf{x})\big(\partial_\tau + M - igA_0(\tau,\mathbf{x})\big)Q(\tau,\mathbf{x}).$$

Because the quark is static, its propagation picks up only two pieces:

$$G_Q(\beta;\mathbf{x}) \propto e^{-\beta M}\,\mathcal{P}\exp\left(ig\int_0^\beta d\tau\, A_0(\tau,\mathbf{x})\right) = e^{-\beta M}\,W(\mathbf{x}).$$

Taking the thermal trace over color then gives the ratio of partition functions with and without one inserted static quark:

$$\frac{Z_Q(\mathbf{x})}{Z} = e^{-\beta M}\left\langle \frac{1}{N_c}\operatorname{Tr} W(\mathbf{x})\right\rangle = e^{-\beta M}\,\langle \ell(\mathbf{x})\rangle.$$

Fitting the Coefficients Using the Lattice Results: IV

(Huang, Reichert, Sannino and Z-W W, PRD **104** (2021) 035005

表: The parameters for the best-fit points.

N	3	$3\ \log$	4	5	6	8
a_0	3.72	4.26	9.51	14.3	16.6	28.7
a_1	-5.73	-6.53	-8.79	-14.2	-47.4	-69.8
a_2	8.49	22.8	10.1	6.40	108	134
a_3	-9.29	-4.10	-12.2	1.74	-147	-180
a_4	0.27		0.489	-10.1	51.9	56.1
b_3	2.40	-1.77		-5.61		
b_4	4.53		-2.46	-10.5	-54.8	-90.5
b_6			3.23		97.3	157
b_8					-43.5	-68.9

The PNJL model Lagrangian (Fukushima, Skokov, PPNP **96** (2017) 154)

- The PNJL Lagrangian can be generically written as:

$$\mathcal{L}_{\rm PNJL} = \mathcal{L}_{\text{pure-gauge}} + \mathcal{L}_{\rm 4F} + \mathcal{L}_{\rm 6F} + \mathcal{L}_k$$

- Without losing generality, we consider below massless 3-flavour case in fundamental representation of $SU(3)$ gauge symmetry
- Here, $\mathcal{L}_{\rm 4F}$ is the four-quark interaction which reads:

$$\mathcal{L}_{\rm 4F} = G_S \sum_{a=0}^{8} [(\bar{\psi}\lambda^a\psi)^2 + (\bar{\psi}i\gamma^5\lambda^a\psi)^2], \qquad \psi = (u,d,s)^T$$

- Six-fermion interaction $\mathcal{L}_{\rm 6F}$ denotes the Kobayashi-Maskawa-'t Hooft (KMT) term breaking $U(1)_A$ down to Z_3 (generically Z_{N_f} for N_f flavours)

$$\mathcal{L}_{\rm 6F} = G_D[\det(\bar{\psi}_{Li}\psi_{Rj}) + \det(\bar{\psi}_{Ri}\psi_{Lj})]$$

Medium Potential: Finite Temperature Contribution

- In the standard NJL model, the medium effect (finite temperature contribution) is implemented by the grand canonical partition function
- In the PNJL model, we can simply do the following replacement to include the contribution from Polyakov loop

$$V_{\text{medium}} = -2N_c T \sum_{u,d,s} \int \frac{d^3p}{(2\pi)^3} \left(\ln\left[1 + e^{-\beta(E-\mu)}\right] + \ln\left[1 + e^{-\beta(E+\mu)}\right] \right)$$

$$\to -2T \sum_{u,d,s} \int \frac{d^3p}{(2\pi)^3} \, \mathrm{Tr}_c \left\{ \left(\ln\left[1 + \mathbf{L}\, e^{-\beta(E-\mu)}\right] + \ln\left[1 + \mathbf{L}^\dagger e^{-\beta(E+\mu)}\right] \right) \right\}$$

- $\mathbf{L}$ is the Polyakov loop:

$$\mathbf{L}(\vec{x}) = \mathcal{P} \exp\left[i \int_0^{1/T} A_4(\vec{x}, \tau)\, \mathrm{d}\tau \right]$$

- In this work, we consider chemical potential $\mu = 0$.

The Constituent Quark Mass and Zero Point Energy: I

(Fukushima, Skokov, PPNP **96** (2017) 154)

- In $\mathcal{L}_{6\mathrm{F}}$, there is also $\langle\bar{u}u\rangle^2\bar{u}u$ term contributes to the constituent quark mass of u
- The total constituent quark mass from $\mathcal{L}_{4\mathrm{F}}$ and $\mathcal{L}_{6\mathrm{F}}$ is:

$$M = -4G_S\sigma - \frac{1}{4}G_D\sigma^2$$

- The expression for the zero-point energy is given by:

$$V_{\mathrm{zero}}\left[\langle\bar{\psi}\psi\rangle\right] = -\dim(\mathrm{R})\,2N_f\int\frac{\mathrm{d}^3p}{(2\pi)^3}E_p\,, \qquad E_p = \sqrt{\vec{p}^2+M^2}$$

  E_p is the energy of a free quark with constituent mass M and three-momentum $\vec{p}$
- The above integration diverges and a regularization is required. We choose a sharp three-momentum cutoff Λ entering the expression for observables and thus also a parameter of the theory.
- Parameters: G_S, G_D, Λ; Observables: M, f_π, m_σ

The Constituent Quark Mass and Zero Point Energy: II

(Fukushima, Skokov, PPNP **96** (2017) 154)

- The integration can be carried analytically and the result is:

$$V_{\text{zero}}\left[\langle\bar{\psi}\psi\rangle\right] = -\frac{\dim(\mathrm{R})N_f\Lambda^4}{8\pi^2}\left[(2+\xi^2)\sqrt{1+\xi^2}\right.$$
$$\left. + \frac{\xi^4}{2}\ln\frac{\sqrt{1+\xi^2}-1}{\sqrt{1+\xi^2}+1}\right],$$

in which $\xi \equiv \frac{M}{\Lambda}$.

The Condensate Energy (Fukushima, Skokov, PPNP **96** (2017) 154)

- In $\mathcal{L}_{4\mathrm{F}}$, the condensate energy then comes from the combination

$$(\bar{\psi}\lambda^0\psi)^2+(\bar{\psi}\lambda^3\psi)^2+(\bar{\psi}\lambda^8\psi)^2=2(\bar{u}u)^2+2(\bar{d}d)^2+2(\bar{s}s)^2$$

- We use the trick is to rewrite $(\bar{u}u)^2$ as

$$\begin{aligned}(\bar{u}u)^2&=\left[(\bar{u}u-\langle\bar{u}u\rangle)+\langle\bar{u}u\rangle\right]^2=(\bar{u}u-\langle\bar{u}u\rangle)^2+2\langle\bar{u}u\rangle\left(\bar{u}u-\langle\bar{u}u\rangle\right)+\langle\bar{u}u\rangle^2\\&\simeq-\langle\bar{u}u\rangle^2+2\langle\bar{u}u\rangle\bar{u}u\,,\end{aligned}$$

  where the $(\bar{u}u-\langle\bar{u}u\rangle)^2$ term is dropped in the spirit of the mean-field approximation.
- The $2\langle\bar{u}u\rangle\bar{u}u$ term contributes to the constituent quark mass of u
- The $-\langle\bar{u}u\rangle^2$ term leads to a contribution to the condensate energy
- Similar procedures can be applied to $(\bar{d}d)^2$ and $(\bar{s}s)^2$, and to $\mathcal{L}_{6\mathrm{F}}$ gives $\langle\bar{u}u\rangle^3$ and we obtain the total condensate energy:

$$V_{\mathrm{cond}}=6G_S\sigma^2+\frac{1}{2}G_D\sigma^3\,,\qquad\sigma\equiv\langle\bar{u}u\rangle=\langle\bar{d}d\rangle=\langle\bar{s}s\rangle=\frac{1}{3}\langle\bar{\psi}\psi\rangle$$

Bubble Nucleation: Chiral Phase Transition (PNJL)

(Reichert, Sannino, Z-W W and Zhang, JHEP **01** (2022) 003, arXiv:2109.11552)

- Chiral phase transition occurs when including fermions
- $\bar{\sigma}$ is classically nonpropagating in PNJL and it's kinetic term is induced only via quantum fluctuations
- We thus include its wave-function renormalization Z_σ with

$$Z_\sigma^{-1} = -\left.\frac{\mathrm{d}\Gamma_{\sigma\sigma}(q^0, \mathbf{q}, \bar{\sigma})}{\mathrm{d}\mathbf{q}^2}\right|_{q^0=0, \mathbf{q}^2=0}, \qquad \Gamma_{\sigma\sigma} = -i\sum 2\,\text{point 1PI}\,\sigma\sigma\,\text{graph}$$

- The three-dimensional Euclidean action and E.O.M. are modified to:

$$S_3(T) = 4\pi\int_0^\infty \mathrm{d}r\, r^2\left[\frac{Z_\sigma^{-1}}{2}\left(\frac{\mathrm{d}\bar{\sigma}}{\mathrm{d}r}\right)^2 + V_{\text{eff}}(\bar{\sigma}, T)\right]$$

$$\frac{\mathrm{d}^2\bar{\sigma}}{\mathrm{d}r^2} + \frac{2}{r}\frac{\mathrm{d}\bar{\sigma}}{\mathrm{d}r} - \frac{1}{2}\frac{\partial \log Z_\sigma}{\partial\bar{\sigma}}\left(\frac{\mathrm{d}\bar{\sigma}}{\mathrm{d}r}\right)^2 = Z_\sigma\frac{\partial V_{\text{eff}}}{\partial\bar{\sigma}}$$

- The associated boundary conditions:

$$\frac{\mathrm{d}\bar{\sigma}(r=0,T)}{\mathrm{d}r} = 0\,, \qquad \lim_{r\to\infty}\bar{\sigma}(r,T) = 0$$

GW parameters α, β and PNJL observables

(Reichert, Sannino, Z-W W and Zhang, JHEP **01** (2022) 003, arXiv:2109.11552.)

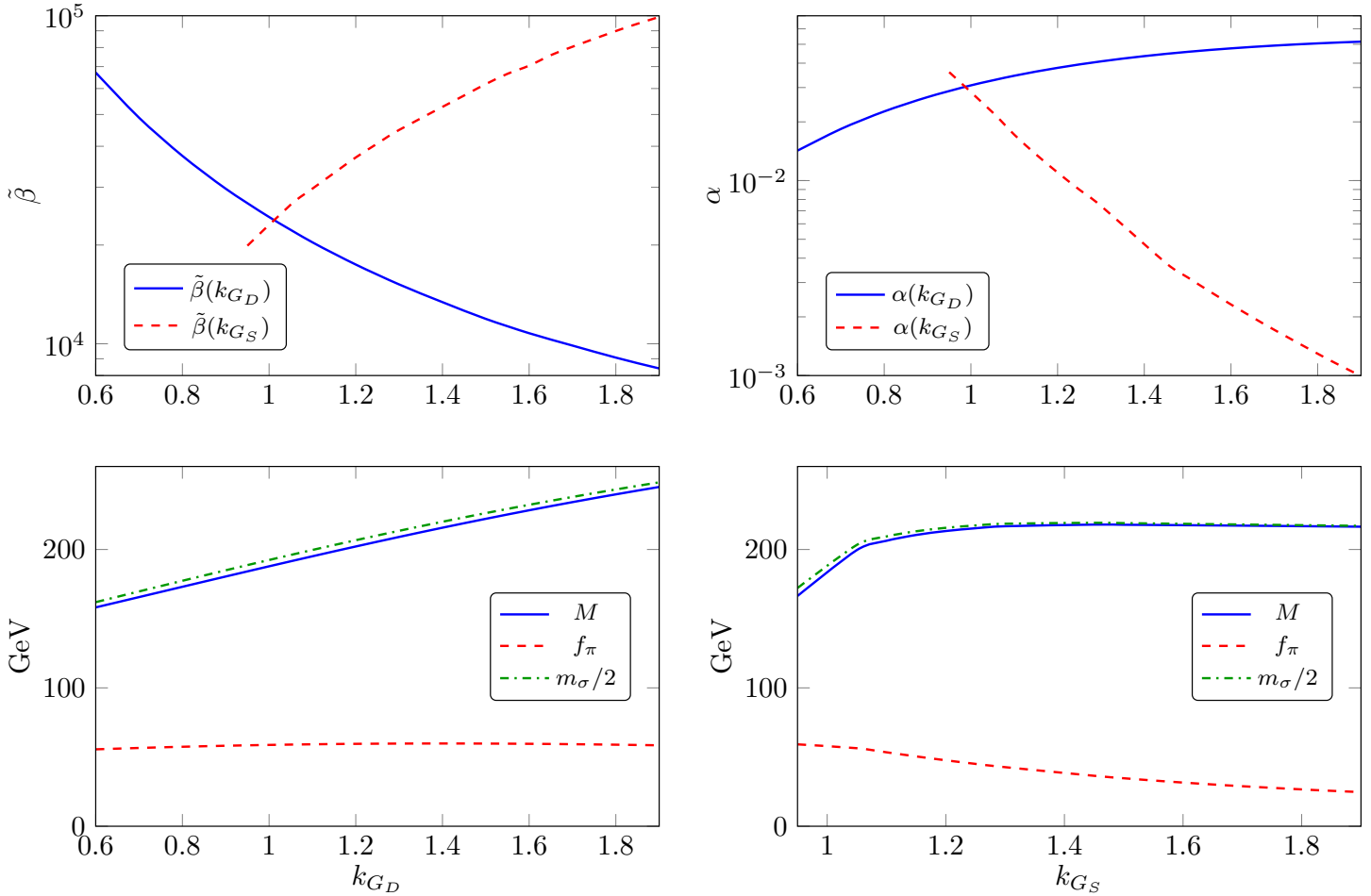

图: The GW parameters $\tilde{\beta}$, α with the observables M, f_π, and m_σ as a function of $G_S = k_{G_S} \cdot 4.6\,\text{GeV}^{-2}$ and $G_D = k_{G_D} \cdot (-743\,\text{GeV}^{-5})$. We use $T_c = 100\,\text{GeV}$, the ratio $\Lambda/T_0 = 3.54$. Below $k_{G_S,\text{crit}} = 0.882$, no chiral symmetry breaking occurs.

Signal to Noise Ratio

(Huang, Reichert, Sannino and Z-W W, PRD **104** (2021) 035005)

$$\mathrm{SNR} = \sqrt{\frac{3\mathrm{year}}{s}\int_{f_{\mathrm{min}}}^{f_{\mathrm{max}}} \mathrm{d}f \left(\frac{h^2\Omega_{\mathrm{GW}}}{h^2\Omega_{\mathrm{det}}}\right)^2}$$

$h^2\Omega_{\mathrm{GW}}$ is the GW spectrum while Ω_{det} is the sensitivity curve of the detector.

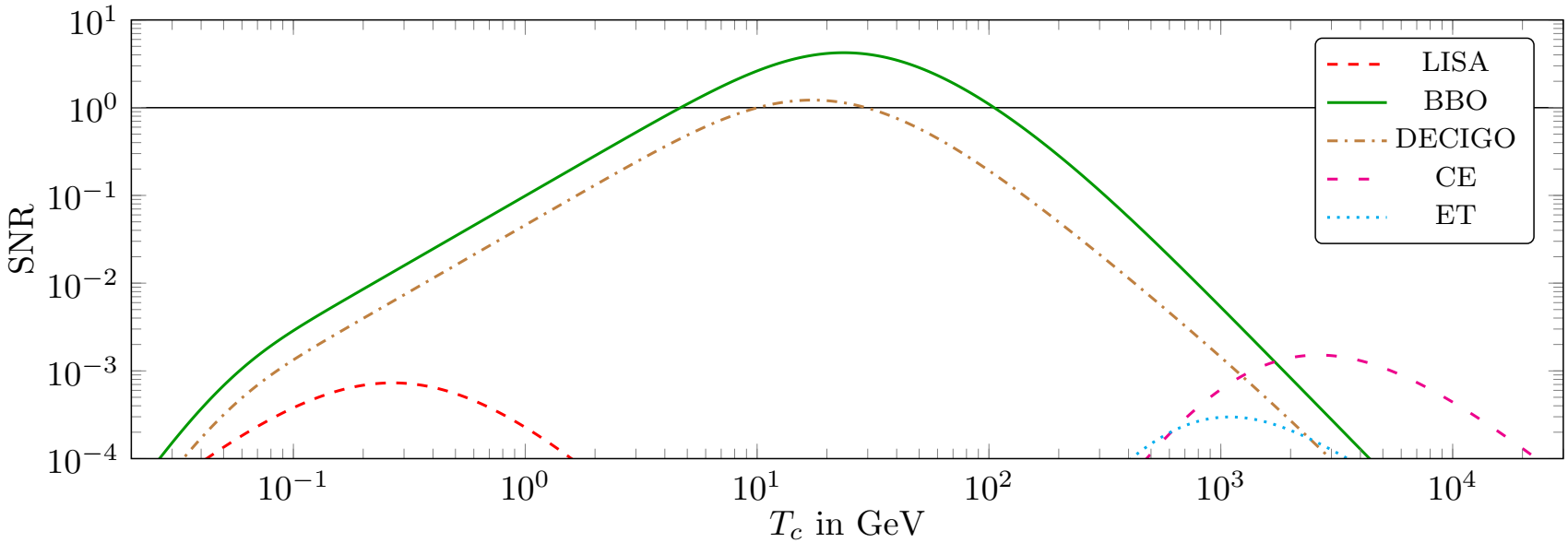

图: We display the SNR for the phase transition in a dark $SU(6)$ sector as a function of the confinement temperature Tc from experiments of LISA, BBO, DECIGO, CE, and ET. We assume an observation time of three years.